Energy Advances

ROYAL SOCIETY OF CHEMISTRY

PAPER

View Article Online
View Journal | View Issue

Cite this: *Energy Adv.*, 2024, 3, 1439

Steady states and kinetic modelling of the acid-catalysed ethanolysis of glucose, cellulose, and corn cob to ethyl levulinate†

Conall McNamara, *[a] Ailís O'Shea,[a] Prajwal Rao,[a] Andrew Ure,[a] Leandro Ayarde-Henríquez,[a] Mohammad Reza Ghaani,[b] Andrew Ross[c] and Stephen Dooley[a]

Ethyl levulinate is a promising advanced biofuel and platform chemical that can be derived from lignocellulosic biomass by ethanolysis processes. It can be blended with both diesel and gasoline and, thus, used in conventional engines and infrastructure. Previously, it has been shown that alkyl levulinate/alcohol/alkyl ether mixtures exhibit significantly enhanced fuel properties relative to any of the individual fuel components, particularly when blended with conventional hydrocarbon liquid fuels. Consequently, this study specifically quantifies the three primary components of the alcoholysis reaction mixture: ethyl levulinate, diethyl ether, and ethanol. The steady state and kinetic phase fractions of ethyl levulinate and diethyl ether produced from glucose, cellulose, and corn cob with 0.5–2 mass% sulphuric acid in ethanol are determined for 5, 10, and 20 mass% of feedstock at 150 °C. Knowledge of the steady state equilibrium mixture fraction is specifically targeted due to its importance in assessing commercial-scale production and in modelling analysis as: (i) it defines the maximum yield possible at a given condition, and (ii) it is equitable to the minimum free energy state. Maximum steady state yields (mass%) of ethyl levulinate of (46.6 ± 3.7), (50.2 ± 5.4), and (27.0 ± 1.9)% are determined for glucose, cellulose, and corn cob, respectively. The conversion of glucose and cellulose to ethyl levulinate in the presence of ethanol and sulphuric acid is shown to be a catalytic process, where the ethyl levulinate yield is not dependent on the acid concentration. For corn-cob biomass, in a new and contrasting finding, the ethyl levulinate yield is shown to strongly depend on the acid concentration. This effect is also observed in the fractions of diethyl ether formed, providing strong evidence that the hydrogen cation is not being replenished in the ethanolysis process and the overall reaction with corncob is not wholly catalytic. Thus, for the acid catalysed alcoholysis of lignocellulosic biomass, acid concentration must be scaled with feedstock concentration. The critical corn cob-to-acid ratio that maximises ethyl levulinate yields while minimizing the formation of undesired co-products (diethyl ether) is in the range 10–20 : 1 at 150 °C. A detailed, hierarchical, mass-conserved chemical kinetic model capable of accurately predicting the relative abundance of the three primary components of the ethanolysis reaction: ethyl levulinate, diethyl ether, and ethanol, from the biochemical composition of the feedstock, is elucidated and validated.

Received 22nd January 2024,
Accepted 2nd April 2024

DOI: 10.1039/d4ya00043a

rsc.li/energy-advances

1. Introduction

The global transportation fleet, encompassing ground, air, and maritime vehicles, heavily relies on fossil-derived fuels, which significantly contributes to anthropogenic greenhouse gas emissions such as CO_2, a major driver of climate change.[1] The substitution of these fuels with biofuels is a viable pathway to mitigate greenhouse gas emissions without the upheaval of existing transportation infrastructure. In this context, two primary challenges confront the industrial upscaling of biofuels. Firstly, the dichotomy of using the crops for either food or fuel production. Additionally, expanding farmland for cultivating crops to increase the production of the latter can pose indirect land-use issues. A feasible solution lies in advanced biofuels, which exclusively utilize non-food waste, residues, and by-products as raw materials. Of the advanced biofuel

[a] School of Physics, Trinity College Dublin, Dublin 2, Ireland. E-mail: mcnamac4@tcd.ie
[b] School of Engineering, Department of Civil, Structural & Environmental Engineering, Trinity College Dublin, Dublin 2, Ireland
[c] School of Chemical and Process Engineering, University of Leeds, 209 Clarendon Road, Leeds LS2 9JT, UK

† Electronic supplementary information (ESI) available. See DOI: https://doi.org/10.1039/d4ya00043a

feedstocks listed in the revised renewable energy directive,[2] lignocellulosic biomass is particularly advantaged as it generally shows high sustainability and, by virtue of its by-product or waste designation, further use of the material is highly desirable. However, lignocellulosic biomass is notably disadvantaged not only in comparison to crude oil products, but also to first-generation biofuels. This is due to the chemically recalcitrant nature of lignocellulose, and its relatively high oxygen content. For fuels, the major share of that oxygen must be removed, requiring energy and technically complicated conversion processes. Energy carriers must compete with incumbent fossil fuels, not only on technical merit, but also on price. Configuring production processes to yield a minimum selling price competitive with what is available for petroleum-derived products is the greatest challenge associated with the deployment of advanced biofuels.[3,4] A technically viable process is insufficient; the process must also be economically viable and competitive with the selling price of crude-oil derived products. This is a severe challenge.

In the specialized literature, a wide range of thermochemical technologies for the conversion of lignocellulosic biomass to advanced biofuels have been reported, including hydrolysis,[5] alcoholysis,[6] pyrolysis,[7] gasification,[8] hydrothermal liquefaction[9] and hydrothermal carbonization.[10] Notably, ''alcoholysis'' (*i.e.*, acid hydrolysis in alcohol solvent) has received relatively limited research attention, underscoring the relevance of this work in quantifying product yields under this process. The primary products of this chemical method are alkyl levulinates, which have been identified as potential drop-in diesel and gasoline biofuels,[11] with extensive additional applications spanning various industrial fields, such as green solvents, platform chemicals (as a precursor to gamma-valerolactone), flavouring agents, lubricants, fragrances, and polymer plasticizers.[12,13]

Upon alcoholysis, the carbohydrates of lignocellulosic biomass undergo a conversion process, forming esters (*i.e.*, alkyl levulinate), while alcohols are converted to ethers (*i.e.*, dialkyl ether).[14] Consequently, the resulting mixture predominantly includes alcohol, alkyl ether, and alkyl levulinate, along with some water and formic acid. Each reaction product stands as a recognised drop-in component for fuel transportation. Nonetheless, the significant limitation to their deployment is the blend-wall behaviour each exhibits when mixed with conventional transportation fuels, marking a substantial challenge in the broad commercial utilization of these biofuels. Howard *et al.*[15] have suggested that mixtures of levulinate ester/alcohol/ether can exhibit fuel properties that are significantly enhanced relative to those of any one of the individual fuel components, in particular when blended with conventional hydrocarbon liquid fuels.[11] They performed critical ignition-quality experiments, revealing the flexible range of fuel properties that are potentially tuneable based on the relative concentration of ethyl levulinate (EL), diethyl ether (DEE), and ethanol in the fuel. These findings effectively delineate the extensive potential compositional space for levulinate ester-based fuels.

Several techno-economic analyses (TEA) have been performed to assess the commercial viability of the alkyl levulinate production through alcoholysis. In particular, Silva and collaborators have conducted a rigorous TEA focusing on the production of ethyl levulinate from lignocellulosic biomass.[16] They analysed 148 individual production process scenarios, identifying fifty-three as the most commercially promising processes. These results hold significant implications for directing future research and development efforts necessary to establish alkyl levulinate as a viable energy carrier, as evidenced by their discoveries: (i) all fifty-three of the most viable processes use sulphuric acid as the catalyst, (ii) the cost of the alcohol (ethanol) is 38% of the expense of the process on average, and (iii) the cost of biomass is 34% of the expense of the process on average. Points ii and iii stress the fundamental relevance of the atom-efficiency within the alcohol and biomass usage, which directly impacts the overall economic feasibility of the process. Point i underscores the unlikely economic feasibility of complex catalysts, regardless of the extensive efforts in different research areas, including mineral acids (Brønsted acids),[17–22] metal salts (Lewis acids),[23–26] ion exchange resins,[19,24,27] sulfonated nanomaterials,[18,24,27–31] polyoxometalates,[30,32–38] zeolites,[22,37,39–43] ionic liquids[44,45] and other miscellaneous nanomaterials.[27,41,43,46–53] Considering Silva *et al.*'s analysis, the reactions investigated in this paper occur in ethanol medium (due to its cost-effectiveness and wider availability compared with bio-butanol[54]) and sulfuric acid.[16]

Knowledge of the steady state equilibrium mixture-fraction is vital for the commercial-scale production of advanced biofuels, as it defines the maximum yield at a given condition and is equitable to the minimum free energy state. However, in the literature, ''yields'' are reported at various reaction times without considering whether the reaction reached the steady state or remained in the kinetic phase. The steady state concentrations of ethyl levulinate from the alcoholysis of lignocellulose have not been empirically established in current literature. Consequently, this work quantitatively determines these concentrations by unveiling the mechanism and rate of diethyl ether formation, a crucial process that is mostly overlooked despite its significant role in alcohol consumption. The second goal is to gain deeper insights into the behaviour of real-world biomass under alcoholysis conditions. The experimental data obtained is methodically integrated into a self-consistent and hierarchical chemical kinetic model, aiming to anticipate the operational behaviour of an alcoholysis system based on the specific biochemical composition of the chosen biomass as the prime feedstock.

2. Theory

2.1. Alkyl levulinate formation

During the alcoholysis of cellulosic biomass, the formation of alkyl levulinates may be notionally summarised by a global reaction of a hexose carbohydrate (*e.g.*, glucose) and alcohol[14]

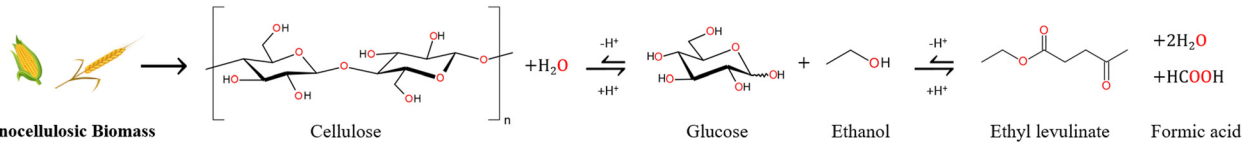

Fig. 1 Reaction mechanism for the production of ethyl levulinate from lignocellulosic biomass.[14] The primary objective of these conversion processes is the elimination of the covalently bounded oxygen atoms (in red) to produce a liquid enriched in hydrogen and carbon, such as ethyl levulinate.

catalysed by a hydrogen cation (proton), as depicted in Fig. 1. In addition to the alkyl levulinate, two molecules of water and a molecule of formic acid may be formed. Note that the formic acid may also react with an additional molecule of alcohol to give the corresponding ester and a further molecule of water. By this simple mechanistic formalism, the hydrogen cation catalyst is regenerated from reactant to product. However, in practice, several other processes are catalysed simultaneously by the proton. The elucidation of the ''catalytic'' nature of this reaction is addressed in this paper.

Insofar assessments of alkyl levulinate production *via* alcoholysis typically assume its formation from the cellulose content of biomass without empirical sustentation, highlighting the limited mechanistic details available. The hemicellulose content could also support alkyl levulinate formation. This study evaluates this hypothesis.

2.2. Dialkyl ether formation

Dialkyl ethers are unavoidable co-products of alcoholysis reactions.[13] The dialkyl ether is formed by the acid-catalysed dehydration of two alcohol molecules accompanied by the formation of one molecule of water, as shown in Fig. 2. It is considered an unwanted side reaction as it consumes the costly alcohol solvent and produces unwanted water in addition to the ether. Ether formation has been noted in some studies but is not reported by the vast majority. Mascal *et al.* showed that 67 mol% of ethanol was converted to diethyl ether in the reaction with dried conifer wood and 2-napthalenesulfonic acid at 200 °C for 4 hours.[55] Furthermore, the study of Silva and co-workers revealed that the cost of the added alcohol represents 38% of the total expenses of the process.[16]

As suggested by Mascal and collaborators and demonstrated by Zhu *et al.*,[56] utilizing lower acid concentrations minimises the formation of diethyl ether. However, this strategy must be further investigated as it reduces the rate of formation of ethyl levulinate.[56] It should be emphasized that the formation of diethyl ether, specifically the relative rate of formation of diethyl ether to the rate of formation of ethyl levulinate is of enormous importance and warrants careful analysis. Despite this, the concentration of the dialkyl ether product is rarely determined. Without this critical information, it is not possible to make an accurate assessment of the overall efficiency or techno-economic viability of the process. Thus, diethyl ether formation is one of the focuses of this paper.

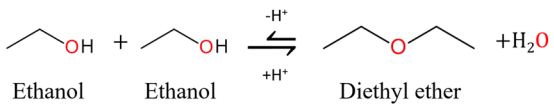

Fig. 2 Reaction mechanism for the acid-catalysed formation of diethyl ether from two molecules of ethanol.[14]

2.3. Humin formation

The hydro/solvothermal reaction of carbohydrates is known to produce insoluble polymeric materials, generically referred to as ''humins''.[57,58] It is speculated that these materials are formed primarily from molecules bearing reactive carbonyl groups (*e.g.*, aldehydes and ketones) that are present in the reaction mixture as a result of the decomposition of the carbohydrate.[57] Recently, Shi *et al.*[57] showed that the formation of humins from glucose in an ethanol medium was inhibited (*i.e.*, no humins detected), compared to the same reaction in water or tetrahydrofuran media where 61 and 53% of the initial carbon was converted to humins, respectively. This inhibition is attributed to the reaction of the aforementioned aldehydes and ketones with the alcohol, thus inhibiting the polymer (humin) formation.[19] This scenario signifies that the production of humins requires meticulous consideration from a techno-economic perspective.

2.4. Water formation

The formation of alkyl levulinates and dialkyl ethers produce water; see Fig. 1 and 2. This is relevant from a techno-economic perspective for two reasons. Firstly, the yield of the esterification reaction is limited by the chemical equilibrium.[16] Therefore, the presence of water, specifically from unwanted competitive processes of dialkyl ether and humin formation, will have adverse effects on the efficiency of the reaction. Secondly, the water content must be removed before the reaction mixture can be used in applications (*e.g.*, as fuel).

2.5. Kinetic model

A chemical kinetic model describes the thermal conversion of reactants into products as a function of time, providing fundamental information on the species concentrations and yields, deepening our understanding of the reaction rates and formation mechanism. This underscores its pivotal role in both the TEA and industrial designing processes. The complexity of lignocellulosic biomass makes the formation mechanism of ethyl levulinate in ethanol difficult to study. The reaction kinetics of ethanol, in the presence of sulfuric acid, with fructose,[59] glucose,[56,60,61] and cellulose,[20] which have previously been explored through a kinetic model, are summarised in the ESI.†

Recently Wang *et al.*[60] combined experiments and quantum chemical calculations to explore the potential energy surface

(PES) describing the thermal conversion of glucose to ethoxymethylfurfural (EMF) and ethyl levulinate catalysed by a hydrogen cation in ethanol solution. It was found that glucose isomerises to fructose before forming hydroxymethylfurfural (HMF), rather than the direct transformation to the latter. Hydroxymethylfurfural converts to ethyl levulinate either *via* ethoxymethylfurfural or levulinic acid (LA). Notably, the pathway leading to EMF is the most thermodynamically favourable. Moreover, the formation of ethyl glucoside from glucose was identified as a parallel reaction. These findings are generally in accordance with the reaction mechanism derived empirically by Flannelly and collaborators.[14] The formation of ethyl glucoside as a crucial intermediate from the ethanolysis of D-glucose has been experimentally supported; however, this observation remains open to theoretical confirmation. It is noteworthy that few studies have used actual lignocellulosic biomass as a reactant; propositions of the reaction mechanism responsible for biomass conversion to ethyl levulinate are consequently unknown.

3. State-of-the-art of ethanolysis

Numerous studies have detailed the acid-catalysed hydrolysis of carbohydrates in other alcohols in a one-pot system. These reports were recently addressed in a comprehensive review by Galletti and co-workers[6] in 2020. In the subsequent Discussion section, Fig. 7–9 present this information, updated to the present day. This analysis is also summarised in the ESI.†

4. Experimental methodology

All materials were acquired from commercial suppliers and used without further purification unless stated otherwise. Ethanol (≥99.8%), ethyl levulinate (99%), sulphuric acid (95–97%), anhydrous dimethyl sulfoxide (≥99.9%), diethyl ether (≥99.8%), and 15 mL Ace Glass pressure vessels were purchased from Sigma-Aldrich, whereas anhydrous D-(+)-glucose (99%) and cellulose (microcrystalline) were purchased from Alfa Aesar. In addition, sodium hydrogen carbonate (≥99.7%) was purchased from Fisher Scientific.

4.1. Corn cob preparation

Corn cobs cleaned of their kernels have become an important reference biomass for advanced biofuel applications. Thus, this study utilizes it as a typical real-world lignocellulosic biomass, compatible with RED II Annex IX.[2] Steamed corn on the cob was purchased from a local supermarket and washed to remove any non-lignocellulosic mass. The corn kernels were removed, and the cob was sliced into ≈2.5 cm pieces. The pieces were weighed and then dried over several days in an oven at 70 °C until no further mass loss was observed. The dried corn cobs were then mechanically broken into smaller pieces and ball-milled for 2 hours. The milling was done using a Glen Creston Spex 8000 mixer/mill with stainless steel balls characterized by a powder charge ratio of 15 : 1.

The resulting powdered corn cob was sieved using a Retsch mesh sieve to isolate and then collect corn cobs of 100–125 μm. These particles were subsequently stored under vacuum in a desiccator until use. For consistency, the D-(+)-glucose and cellulose feedstocks were also sieved to a particle size of 100–125 μm.

4.2. General reaction procedure

Feedstock, ethanol, and sulfuric acid were added to a 15 mL pressure tube with a magnetic stirrer. The total mass of the three reactants was set at 5 grams, and the percentage mass of each reactant was adjusted according to the desired reaction conditions. The pressure tube was tightly sealed and placed in an insulated aluminium heating block at 150 °C for the desired reaction time. The heating block was insulated with a 2.5 cm layer of Styrofoam covered with tin foil that enclosed all sides of the block. After completion, the pressure tube was placed in a Teflon rack and air-cooled to guarantee that the contents returned to the condensed phase.

The mixture was centrifuged at 5500 revolutions per minute for 7 minutes at room temperature. Centrifugation was performed on a ThermoScientific TM Sovall TM ST 8 small benchtop centrifuge with a ThermoScientific Tm HIGHConic TM III fixed angle rotor. The solid residue removed *via* this process may contain both unreacted feedstocks as well as humins formed during alcoholysis. After the supernatant had been separated, the reaction was neutralised using 50 milligram of sodium hydrogen carbonate.

Two separate reactions were performed for each set of conditions and two gas chromatography samples were prepared for each reaction. This procedure produced 4 data points for each set of reaction conditions.

4.3. "Yield" calculations from global chemical reactions

The known mechanism of the global acid-catalysed reaction yielding ethyl levulinate can be reasonably generalised as follows:

Glucose:

$$C_6H_{12}O_6 + C_2H_5OH + H^+ \leftrightarrow C_7H_{12}O_3 + 2H_2O + HCOOH + H^+ \quad (1)$$

Cellulose:

$$(C_6H_{10}O_5)_n + nC_2H_5OH + H^+ \leftrightarrow nC_7H_{12}O_3 + nH_2O + nHCOOH + H^+ \quad (2)$$

Corn cob:

$$Y(C_6H_{10}O_5)_n + YnC_2H_5OH + H^+ \leftrightarrow YnC_7H_{12}O_3 + YnH_2O + YnHOCOH + H^+ \quad (3)$$

Diethyl ether:

$$C_2H_5OH + C_2H_5OH + H^+ \leftrightarrow C_2H_5OC_2H_5 + H_2O + H^+ \quad (4)$$

where Y is the mass fraction of cellulose in the corn cob sample.

These relations reveal that the maximum potential yield of ethyl levulinate is directly correlated with the number of the

added carbohydrate fraction, regardless of their specific form, *e.g.*, glucose, fructose, cellulose, or raw biomass. Notably, the accuracy of the outlined global reactions profoundly influences the resulting yield values, a principle extending to previous works reporting yield percentages. Accurate assignment of these values necessitates a comprehensive understanding of the underlying reaction mechanism, a subject formally stated in the Kinetic model section of this study.

Ideally, the alcoholysis yields achieved would be expressed in molar form. However, to perform this calculation for real-world biomass, several assumptions must be made. Firstly, all ethyl levulinate produced must be assumed to come from the cellulose portion of the biomass. This is an unrealistic assumption and is contested in this paper. Secondly, the molar yield would be dependent on the accuracy of the biochemical analysis and would thus naturally embody an additional uncertainty.

Therefore, the ethyl levulinate yield was approximated as the fraction between its mass and the mass of the feedstock added (glucose, cellulose, or corn cob). This simplification, although arbitrary, seems reasonable and, more importantly, disregards unrealistic assumptions.

$$\text{Yield of ethyl levulinate}\,(\%) = \frac{\text{Ethyl levulinate formed}\,(\text{g})}{\text{Feedstock added}\,(\text{g})} \times 100\% \quad (5)$$

4.4. Gas chromatography analysis

Following quenching, an aliquot of the liquid-phase reaction mixture was carefully sampled and assessed *via* gas chromatography (GC). All samples were prepared on gravimetric basis as an aliquot of the reaction mixture (500 mg) was diluted in dimethyl sulfoxide (DMSO) such that the mass ratio of DMSO to the reaction mixture was 400 : 1. The mass of DMSO needed was recorded. Then, the solution was transferred to a crimp top vial for GC analysis. Such an analysis was performed on a PerkinElmer Clarus 580, GC-FID, equipped with an Agilent DB-624 column (30 m, 320 μm i.d., 1.80 μm film) using the TotalChrom 6.3.2 software package (MA, USA). Hydrogen was used as the carrier gas, with a constant flow of 2 mL min^{-1}. The inlet temperature was maintained at 493.15 K with the detector set to 543.15 K. A sample volume of 1 μL was injected at a split of 40 : 1. The oven conditions were: 348.15 K for 2 minutes, 10 K min^{-1} to 423.15 K; 20 K min^{-1} to 443.15 K, 10 K min^{-1} to 493.15 K.

4.5. Feedstock analysis. Ultimate analysis

Ultimate analysis was conducted to measure the elemental content of carbon (C), hydrogen (H), and nitrogen (N) in the samples using a Flash 2000 CHNS Analyzer from Thermo Scientific. The instrument was checked/calibrated using both calibration standards and certified biomass reference materials from elemental microanalysis (UK). About 3 mg of the sample was weighed into a tin capsule in duplicates, and trapped air was squeezed out as much as possible by carefully crimping the capsule containing the weighed sample. The sample is dropped in the Flash 2000 CHNS analyser preheated to 900 °C in a continuous stream of helium. A known quantity of oxygen is then briefly added, and the sample burns. The combustion products are further processed in an oxidation/reduction reactor to be in the desired form of CO_2, H_2O, and N_2, then separated with a gas chromatography column and lastly measured by means of thermal conductivity detection.

4.6. Steady state conditions and uncertainties

From thermodynamics, a reaction will proceed until the product and reactants are present at concentrations that minimise the (Gibb's) free energy of the system according to:

$$\Delta G_0 = -RT \ln K_{\text{eq}} \quad (6)$$

where ΔG_0 is the standard state Gibb's free energy, R the gas constant, T is the temperature, and K_{eq} the reaction quotient at equilibrium (*i.e.*, the equilibrium constant). The equilibrium mixture fraction is a pivotal parameter in the validation of physics-based analysis, that may be used to assess the techno-economic viability of a process, such as kinetic models. It is our thesis that these models can and should have basic theoretical underpinning, such as the conservation of elemental mass and validity to thermodynamic equilibrium.

For this purpose, it is important to measure the mass of reactant, product, and co-products in as far as is possible (ethanol, ethyl levulinate, diethyl ether, humins and, if possible, water) as this determines the theoretical maximum yield of the process, with the inclusion of the influence of molecular thermodynamics. Thus, such experimental data can be used to inform the fundamental quantities of eqn (6), extending the validity of a model beyond the specific experimental study it has been developed with. Therefore, steady state fractions of reactants, products, and co-products and the formation time required are specifically targeted as information by which to characterise and numerically model the synthetic process. For this purpose, the time at which steady state occurs must be objectively defined. We suggest the shortest reaction time at which the mass of ethyl levulinate is constant within experimental uncertainty (typically ± 10%) across three consecutive time points.

4.7. Reproducibility and repeatability

Experiments and gas chromatography analyses were replicated under the same conditions to guarantee the reproducibility of the tests. Duplicate experiments were performed for every set of reaction conditions, and duplicate gas chromatography analyses were performed for each experiment, thus giving four data points for every set of reaction conditions. The uncertainties presented for the data points on the graphs are the standard deviations of the four data points at those experimental conditions. The uncertainties of the steady state concentrations and yields are the standard deviations of data points satisfying the equilibrium conditions (32–40 data points).

4.8. Hierarchical mass conserved chemical kinetic modelling

A chemical kinetic model for the acid-catalysed ethanolysis of glucose, cellulose, and corncob was developed to evaluate the

applicability of the global chemical eqn (1)–(4) above, providing a basic comprehension of the reaction mechanism with associated kinetics.

4.8.1. Hierarchical elemental mass conserved reaction mechanism. Given the ubiquitous chemical structure of monosaccharides across various biomasses, a hierarchical learning approach is a valuable concept for managing the chemical complexity of biomasses and equating its reaction behaviour to fundamentals. Given the commonality in chemical structure, the reaction behaviours and kinetics observed in glucose can be extrapolated to cellulose, and those of cellulose extrapolated to lignocellulose (*e.g.*, corn cob). An obvious but important physical imposition here is that of mass conservation. Each reaction incorporated in the kinetic model is mass conservative. This provides an important mathematical constraint when deriving the "optimal" kinetic constants from experimental observations and also in deducing what reaction mechanism best describes those observations and, therefore, which global chemical reactions most fairly summarise the system.

Table 4 and Fig. 3 list a collection of reactions, hierarchically constructed considering one submodel at a time: diethyl ether, glucose, cellulose, and finally, corncob. The dehydration of ethanol to diethyl ether is studied in parallel with each submodel. Due to the unknown nature of the system, this reaction network was proposed based on the major species detected. Fig. 3 shows mass-conserved reactions comprising the kinetic model proposed for the ethanolysis of glucose, cellulose, and corncob. Reactions (3)–(9) were optimised to all glucose data. Reactions (10)–(13) were optimised with the addition of cellulose data. Reactions (14)–(18) were optimised with the addition of corncob data. The composition of unknown variables is dependent upon the source species and the catalytic nature of the reaction under consideration.

4.8.2. Diethyl ether. The oversight of diethyl ether as a significant co-product in literature studies of the alcoholysis process is a major shortcoming of previous kinetic models for ethanolysis. This gap in understanding contributes to the present limitation in performing an accurate TEA of ethyl levulinate production. In this study, the condensation reaction of ethanol to diethyl ether is represented as an acid-catalysed, reversible reaction. This submodel also includes the protonation and deprotonation of ethanol and water.

4.8.3. Glucose. The conversion of monosaccharide glucopyranose to ethyl levulinate is modelled to proceed through the intermediate ethyl glucopyranoside. This is the main experimentally observed pathway.[61] Humins resulting from glucose ethanolysis is modelled *via* the formation of "$Unknown_{Glucose}$" from both glucopyranose and ethyl glucopyranoside.

4.8.4. Cellulose. The more complex cellulose molecule is modelled to depolymerise *via* two reaction pathways due to the presence of both ethanol and water in the reaction system: (i) an acid hydrolysis pathway and (ii) an acid ethanolysis pathway. Cellulose is either depolymerised along the acid hydrolysis pathway to form glucopyranose or throughout the acid ethanolysis pathway to produce ethyl glucopyranoside. Humin formation from cellulose ethanolysis is modelled through the production of "$Unknown_{Cellulose}$".

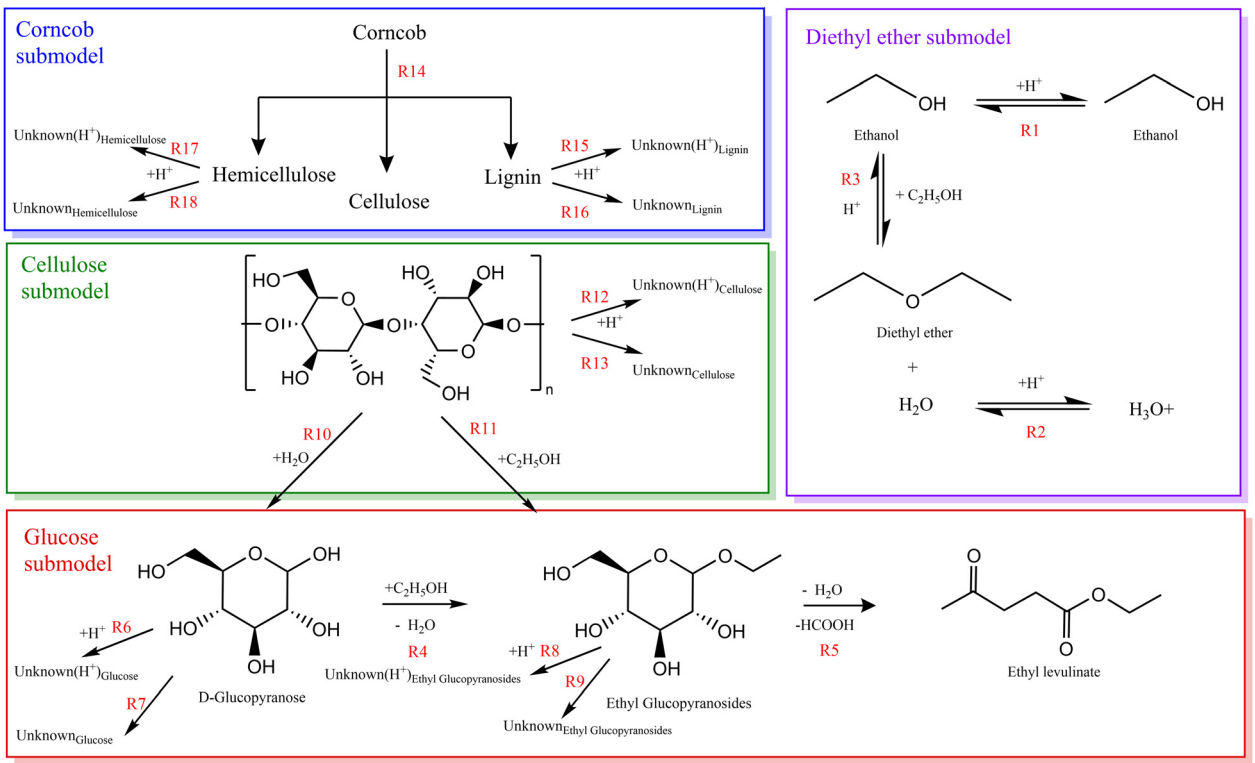

Fig. 3 Proposed chemical kinetic model, and set of sub-models, detailing the reaction mechanism of corncob, cellulose, and glucose to produce ethyl levulinate under sulphuric acid-catalysed ethanolysis conditions.

4.8.5. Corn cob. Corn cob is a typical real-world lignocellulosic biomass. Modelling the chemical reaction of such lignocellulosic matter requires resolving the challenge presented by its complex and variable chemical composition. To achieve this, the concept of a surrogate is proposed, where a surrogate is a synthetic composition of each of the main biopolymers comprising any lignocellulosic biomass, (cellulose, hemicellulose, and lignin), where each fraction is matched to the respective fraction comprising the actual lignocellulose in question.

Within this framework, in the absence of better information, the lignocellulose is assumed to instantaneous depolymerise to the respective fractions of cellulose, hemicellulose, and lignin, at the mass ratio learned from biochemical analysis (*i.e.*, for corncob 40.8 : 46.7 : 12.5, cellulose: hemicellulose: lignin).[62] The molecular composition of cellulose and hemicellulose are defined in terms of the monomeric units, n, $(C_6H_{10}O_5)_n$ and $(C_5H_8O_4)_n$, respectively, which is consistent with the dehydrated repeating monomeric structures of glucose and xylose.[63,64] The experimental measurement of the mass fraction of each biopolymer allows for the determination of the value of n. The definition of a standardized unit of corn cob is based on a stoichiometric analysis, allowing this unit to decompose into one monomer of cellulose and therefore 0.882 monomers of hemicellulose. This facilitates the composition of lignin to be inferred from the remaining elemental balance of the corn cob.

4.8.6. "Unknowns". Both non-catalytic and catalytic pathways are modelled to produce "Unknowns" from each intermediate, which are essential to describe the partial consumption of the acid and the formation of humins and other soluble species ("Unknowns"). The elemental compositions of humins were determined experimentally to have an approximate carbon-to-hydrogen molar ratio of 1 : 1. Consequently, this ratio is used as the molecular composition of "Unknowns" in the model. Furthermore, it is assumed that "Unknowns" formed from lignin maintain a consistent molar ratio to the initial structure and this process yields between 0 and 4.5 water molecules. The oxygen content of each "Unknown" species is inferred from arithmetic involving its precursor intermediate and the number of water molecules produced.

4.8.7. Kinetic model optimisation. A hierarchical approach was employed for optimising the kinetic constants to experimentally derived values. Each submodel was optimised to time-resolved experimental data for the corresponding feedstock component using the Phase 1 module of the MLOCK coded-algorithm[65] under two postulates: i. the system is isobaric and homogeneous, and ii. the sulfuric acid fully dissociates at the reaction temperature. Our group has developed this algorithm to optimize kinetic models for the pyrolysis of hemicellulose and lignin through the generation and evaluation of sets of solutions by simultaneous perturbation of Arrhenius parameters. The submodels were optimised in ascending order according to their chemical complexity, *i.e.*, diethyl ether, glucose, cellulose, and corncob. Once derived, the rate constants for each submodel were held constant in the overall system during subsequent optimisations.

A set of ordinary differential equations were used to describe the concentrations of the species in the system as a function of time, as exemplified for glucopyranose:

$$\begin{aligned}\frac{\mathrm{d}[\text{glucopyranose}]}{\mathrm{d}t} &= k_{10}[H_3O^+][\text{cellulose}] \\ &\quad - (k_4)[C_2H_5OH_2^+][\text{glucopyranose}] \\ &\quad - (k_6 + k_7)[H^+][\text{glucopyranose}]\end{aligned} \tag{7}$$

where k_{10} is the rate constant to produce glucopyranose from cellulose, k_4, k_6, and k_7 represent the conversion rate of glucopyranose to ethyl glucoside, "Unknown$(H^+)_{\text{Glucose}}$", and "Unknown$_{\text{Glucose}}$", respectively. In the first iteration, these constants were collected from the literature.[66] Then, the system of differential equations was solved numerically using Cantera. The discrepancies between the concentration predicted by the model and the corresponding experimental value of the key species were calculated using least square errors, averaged across each experimental condition:

$$\text{Error}_i = \sum_{\text{All exp conditions}} \frac{\sum_{t=0}^{t_f} \left(\frac{x^t_{\text{exp},i} + x^t_{\text{model},i}}{x^t_{\text{exp}}} \right)^2}{N_{x_{\text{exp}}}} \tag{8}$$

where $x^t_{\text{exp},i}$ is the mass of species i measured experimentally after time t, $x^t_{\text{model},i}$ stands for the mass of species i calculated by the model after time t, and $N_{x_{\text{exp}}}$ represents the number of experimental data points.

By varying the rate constants input into the model, an objective error function was calculated. The minimum of the error function was found, and the corresponding rate constants were selected as the empirical rate constants, which allows for the best reproduction of the experimental data. Tables 4 and 5 show the rate constants derived from the optimisation of the kinetic model and the overall fidelity of the model to reproduce the mass of ethyl levulinate, diethyl ether, and humins formed experimentally. The rate constants from the reaction of glucose in ethanol (k_3–k_9) are first optimised and are then held constant in the model in order to derive the subsequent rates of the reaction of cellulose in ethanol (k_{10}–k_{13}). These rate constants are similarly held constant to derive the final rates for the reaction of corncob in ethanol (k_{15}–k_{18}). The corresponding model's predicted species concentrations are discussed in the results section.

4.8.8. Fidelity index. A fidelity index was calculated to assess the overall chemical performance of the model. To accurately assess how well the chemical kinetic model predicts the real-world kinetics of this process, the fidelity index includes two terms: an R^2 term and a mass-conservation term. The R^2 metric measures the degree of exactness captured by the model in terms of experimental reproducibility, whereas the mass-conservation term assesses the mass fraction quantified after the longest reaction time-point (*i.e.*, 10 000 minutes) relative to the initial reactant's mass. This fidelity index is thus defined as:

$$\text{Fidelity index} = \text{RMS}\left[R_{\text{EL}}{}^2, R_{\text{DEE}}{}^2, R_{\text{EtOH}}{}^2\right] \times \frac{\text{EL(g)} + \text{Ethanol(g)} + \text{DEE(g)} + \text{EL(mol)}\left(2 \times M_{\text{H}_2\text{O}} + M_{\text{HCOOH}}\right) + \text{DEE(mol)}\left(M_{\text{H}_2\text{O}}\right)}{\text{Feedstock(g)} + \text{Ethanol(g)}} \quad (9)$$

where M refers to the molecular weight of the relevant species and RMS the root-mean-square.

5. Results and discussion

5.1. Composition of raw materials

To determine the moisture content of cobs of corn, eight stalks of steamed corn were purchased at a city supermarket. Each cob is cleaned completely of all kernels and dried in an oven set to a controlled temperature of 50 °C. The weights of each cob are continuously measured over the course of 256 hours. Considering the inhibitor effects of water on the ethyl levulinate formation, all corn cobs are continuously dried at 50 °C and weighed every day until no change in mass is observed. The moisture content of the 8 cobs studied is in the range of (67.5 to 81.1) mass%, while the average of corn cob is (74.8 ± 4.7) mass%.

5.1.1. Feedstock analysis. Table 1 presents the elemental analysis for glucose, cellulose, corn cob, and other promising ANNEX IX feedstocks for advanced biofuel production listed in RED II.[2]

Table 1 Ultimate analysis (mass%) of dried feedstocks

Feedstock	Mass% carbon	Mass% hydrogen	Mass% nitrogen	H/C mole ratio
Glucose	40.0	6.7	0.0	2.00
Cellulose	42.0	6.1	0.0	1.73
Corn cob	43.3	5.8	0.6	1.61
Wheat straw	43.4	5.4	0.4	1.51
Barley straw	42.3	5.3	0.4	1.51
Oat straw	41.8	5.3	0.8	1.51

5.2. Steady state analysis of the ethanolysis of glucose, cellulose, and corn cob

The steady state times, concentrations, and yields of ethyl levulinate recorded for the sulphuric acid-catalysed (0.5 mass%) ethanolysis of glucose, cellulose, and corn cob at 5, 10, and 20 mass%, at 150 °C, are listed in Table 2.

Because of the chemical complexity, the observed steady state times of ethyl levulinate's production are the following: glucose <1000, cellulose <2000, and corn cob <3000 minutes. This trend is integrated into the construction of the kinetic model in the form of sub-models. For a given reaction time and initial concentration of the feedstock, the concentration of ethyl levulinate formed is observed to be dependent on the feedstock type. The concentration of ethyl levulinate obtained from the alcoholysis of glucose and cellulose is approximately double that obtained from corn cob. This yield of ethyl levulinate from corn cob is higher than that predicted based on the cellulose content of the corn cob and the experimentally determined ethyl levulinate yields from pure cellulose. This discovery indicates that ethyl levulinate may also be derived from other constituents of the lignocellulosic biomass, such as hemicellulose, and challenges the common assumption that all ethyl levulinate produced from the alcoholysis of real-world biomass is derived from its cellulose content.

The highest average steady state concentrations of ethyl levulinate produced from the ethanolysis of glucose and cellulose are achieved at the highest mass loading of the feedstock (20 mass%): (0.41 g ± 0.07) g, *i.e.*, (40.8 ± 7.3)% yield, and (0.40 g ± 0.06) g, *i.e.*, (39.7 ± 6.1)% yield, respectively. A clear dependence is observed between the ethyl levulinate (g) formed and the initial mass loading of the feedstock for both glucose

Table 2 Steady states of ethyl levulinate production

Feedstock	Mass of feedstock (mass%)	Acid concentration (mass%)	Average steady state mass of ethyl levulinate (g)	Ethyl levulinate yield (mass%)	Time to reach steady state (min)
Glucose	5	0.5	0.12 ± 0.01	46.6 ± 3.7	500–1000
	10		0.23 ± 0.01	45.0 ± 2.7	
	20		0.40 ± 0.07	40.4 ± 6.7	
Cellulose	5	0.5	0.13 ± 0.01	50.2 ± 5.4	1000–2000
	10		0.24 ± 0.03	48.3 ± 5.7	
	20		0.39 ± 0.08	38.9 ± 7.5	
Corn cob	5	0.5	0.07 ± 0.01	27.0 ± 1.9	2000–3000
	10		0.11 ± 0.01	21.4 ± 2.7	1000–2000
	20		0.06 ± 0.02	6.3 ± 1.5	2000–3000
	20	2.0	0.20 ± 0.05	19.6 ± 4.8	2000–3000

Average steady state masses, average steady state yields and time taken to reach steady state for ethyl levulinate production *via* sulphuric acid catalysed ethanolysis (according to the previously defined conditions to achieve steady state) for the three loadings of each of the three feedstocks at 150 °C. Uncertainty = 1 standard deviation.

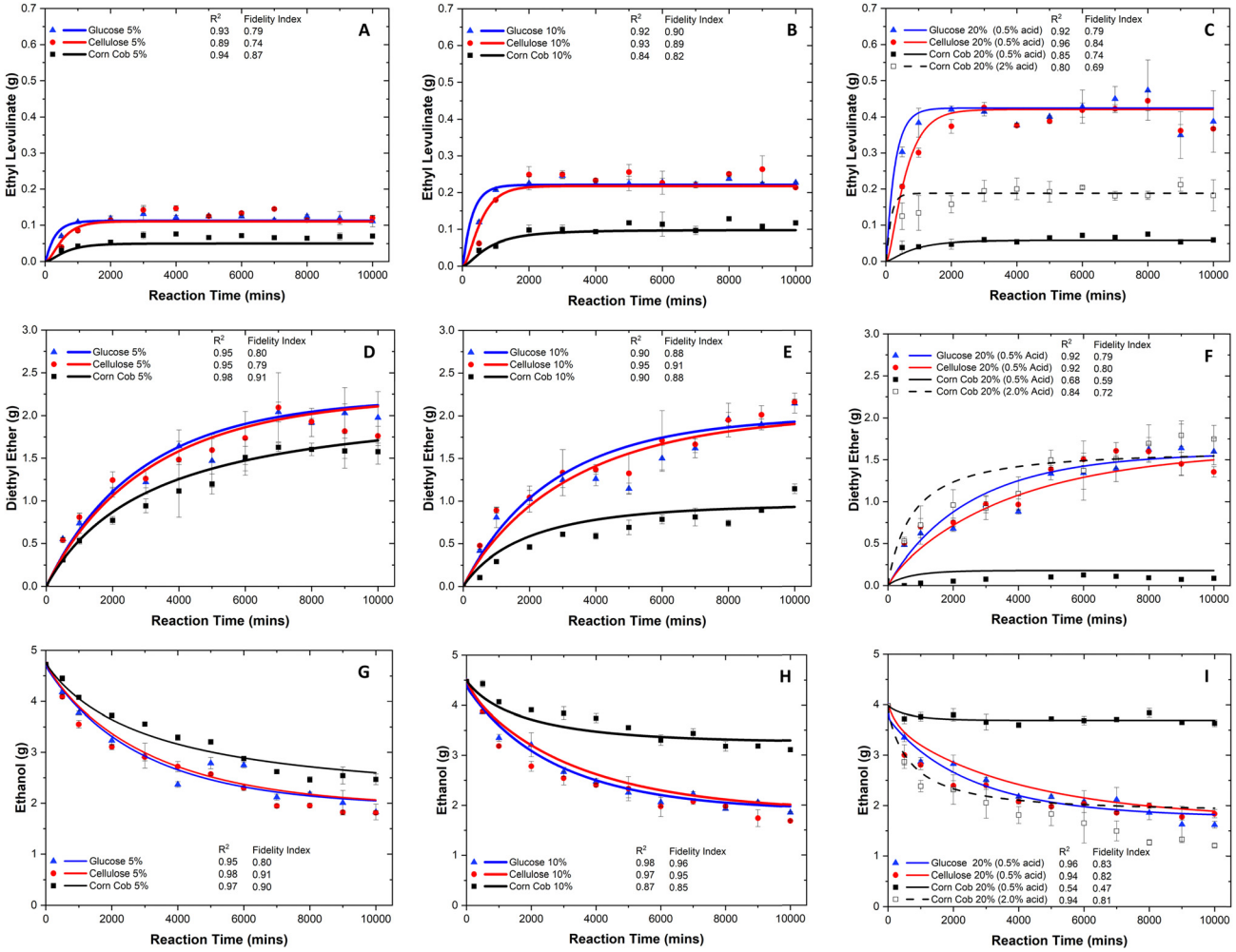

Fig. 4 Ethyl levulinate (g) [A–C], diethyl ether (g) [D–F], and ethanol (g) [G–I] concentrations present in the product mixture produced from the sulphuric acid-catalysed ethanolysis of glucose, cellulose, and corn cob (5, 10, and 20 mass%) at 150 °C. The data points represent the average of 4 experimental data points, while the error bars are the standard deviation of those 4 points. The lines are produced by the chemical kinetic model.

and cellulose. Surprisingly, this trend is not observed for corn cob, a real-world lignocellulosic biomass.

The amount of ethyl levulinate produced from the ethanolysis of corn cob, with 0.5 mass% acid, scales linearly with the initial mass loading of feedstock until some critical value above 10 mass% of feedstock. Initially, the maximum steady state concentration achieved for corn cob is (0.10 ± 0.02) g, *i.e.*, (20.3 ± 3.5)% yield, by utilizing 0.5 mass% of acid at 10 mass% of feedstock. Conversely, the ethyl levulinate formed for 20 mass% of corn cob was only (0.06 ± 0.02) g, *i.e.*, (6.3 ± 1.5)% yield. This could be triggered by the changing feedstock to acid ratio, as the sulphuric acid concentration is kept constant (0.5 mass%). Therefore, an additional time-dependent data set for corn cob (20 mass%) with a higher acid concentration (2 mass%) is performed to improve the yield of ethyl levulinate, leading to (0.20 ± 0.05) g, *i.e.*, (19.6 ± 4.8)% yield. This shows that the ethyl levulinate production from corn cob requires the acid concentration to be scaled with the biomass concentration, indicating that the process is not fully catalytic. To investigate the catalytic nature of lignocellulosic alcoholysis, another set of acid-dependent experiments are performed and are discussed in the next section.

The highest average steady state yields of ethyl levulinate produced from the ethanolysis of glucose (46.6 ± 3.7), cellulose (50.2 ± 5.4), and corn cob (27.0 ± 1.9) mass% are achieved at 5 mass% feedstock, 0.5 mass% sulphuric acid, and 94.5 mass% ethanol at 150 °C. Notably, the yield of ethyl levulinate decreases as the feedstock loading increases. This trend tends to result in studies configuring a lower feedstock concentration relative to the ethanol and acid concentrations to achieve maximum yields of ethyl levulinate. It is important to appreciate the techno-economic realities when considering the commercialisation of such a process. While lower feedstocks loadings may result in higher ethyl levulinate yields, this also results in greater use and consumption of the costly alcohol, which accounts for approximately 38% of the total process.[16]

This trend is amplified for corn cob as there is a significant drop in ethyl levulinate yield as the feedstock loading increases. The yield drops from 27.0 to 6.3% at 5 and 20 mass% of corn cob, respectively. This indicates that protons are irreversibly

consumed at higher concentrations of biomass relative to the sulphuric acid, preventing the reaction from proceeding. These findings are illustrated in Fig. 4. This hypothesis is further evidenced by the quantities of diethyl ether present in the reaction mixture. For glucose and cellulose, a small drop in diethyl ether production is observed, as the feedstock loading increases. This is due to the decrease in concentration of ethanol in the reaction as the formation of diethyl ether is both a function of initial acid and ethanol concentrations. Therefore, a small drop in diethyl ether production is expected for these reaction conditions. However, at 20 mass% of corn cob, a negligible quantity of diethyl ether is produced. This again indicates that for the real lignocellulosic biomass, corn cob, the hydrogen cation is being consumed in some irreversible process so that the reaction cannot proceed, indicating that the reaction is not wholly catalytic.

5.3. Effect of acid concentration on yields

A series of experiments are performed to determine the effect of acid concentration on the alcoholysis of biomass to produce ethyl levulinate at three different feedstock : acid ratios (10 : 1, 20 : 1, and 40 : 1) and feedstock loadings (5, 10, and 20 mass%) for glucose, cellulose, and corn cob; see Table 3. Two sets of experiments are carried out to evaluate the catalytic nature of this system at a constant mass mixture of 5 g: one at steady state conditions (reaction time of 6000 minutes) and one at kinetic phase conditions (reaction time of 1000 minutes), as shown in Fig. 5.

At 6000 minutes, when the reaction is at steady state, the amount of ethyl levulinate formed from glucose and cellulose is independent of the acid concentration. This is also true for glucose at 1000 minutes, as this reaction has reached its steady state at this point. This further supports the catalytic features of this process driven by the regeneration of hydrogen cations.

Table 3 Acid-dependent study of ethyl levulinate production at 6000 minutes

Feedstock	Feedstock (mass%)	Feedstock : acid mass ratio 10 : 1	20 : 1	40 : 1
		Steady state ethyl levulinate yields (mass%)		
Glucose	5	46.5 ± 1.7	53.4 ± 6.1	45.4 ± 10.3
	10	41.6 ± 2.5	43.4 ± 5.7	51.3 ± 12.7
	20	41.7 ± 2.6	41.5 ± 5.4	39.4 ± 1.8
Cellulose	5	49.2 ± 2.1	51.0 ± 4.1	40.7 ± 5.8
	10	43.0 ± 1.5	42.9 ± 1.3	53.3 ± 18.5
	20	43.1 ± 3.1	39.9 ± 4.1	41.4 ± 1.0
Corn cob	5	26.2 ± 2.2	13.0 ± 1.0	3.7 ± 1.4
	10	23.9 ± 4.0	22.4 ± 4.6	5.8 ± 0.4
	20	20.6 ± 5.3	18.9 ± 0.2	6.4 ± 0.3

Yields (mass%) of ethyl levulinate produced from the sulphuric acid-catalysed ethanolysis of glucose, cellulose, and corn cob (5, 10, and 20 mass percent) for three different feedstock-to-acid ratios (10 : 1, 20 : 1, and 40 : 1) at 150 °C for a reaction time of 6000 minutes. Four experiments are performed for each data point, and the error is the standard deviation of those four points.

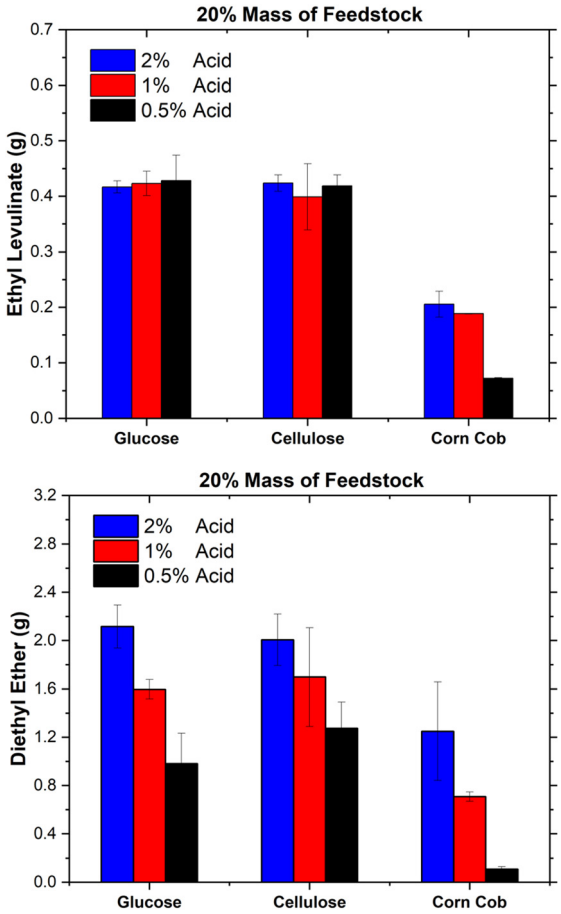

Fig. 6 Ethyl levulinate (g) and diethyl ether (g) produced from the sulphuric acid-catalysed ethanolysis of glucose, cellulose, and corn cob (5, 10, and 20 mass %) for three different feedstock-to-acid ratios (10 : 1, 20 : 1, and 40 : 1) for a reaction time of 6000 minutes at 150 °C.

However, for cellulose at 1000 minutes, the reaction is still in the kinetic phase, meaning that the steady state has not been reached. At this point, the ethyl levulinate formed is dependent on the acid concentration, indicating that the concentration of acid appears to only affect the rate of the reaction but not the concentration of ethyl levulinate in steady states.

For corn cob at 6000 minutes, the amount of ethyl levulinate formed is dependent on the concentration of acid until some critical value. At a feedstock:acid ratio of 40 : 1, the amount of ethyl levulinate and diethyl ether is negligible, evidencing the population of protons is too low to catalyse the reactions as they are consumed *via* an unexplored mechanism. Diethyl ether is an unavoidable co-product in the acid-catalysed ethanolysis of biomass. As shown in Fig. 6, the produced amount of this species is dependent on the acid content added to the system. It is, therefore, desirable to use the minimum concentration of acid necessary in order to minimise diethyl ether production. The determination of this minimum concentration for the case of sulphuric acid is essential for the TEA of such a process. For corn cob at 150 °C, this feedstock:acid ratio is in the range of 10 : 1 to 20 : 1.

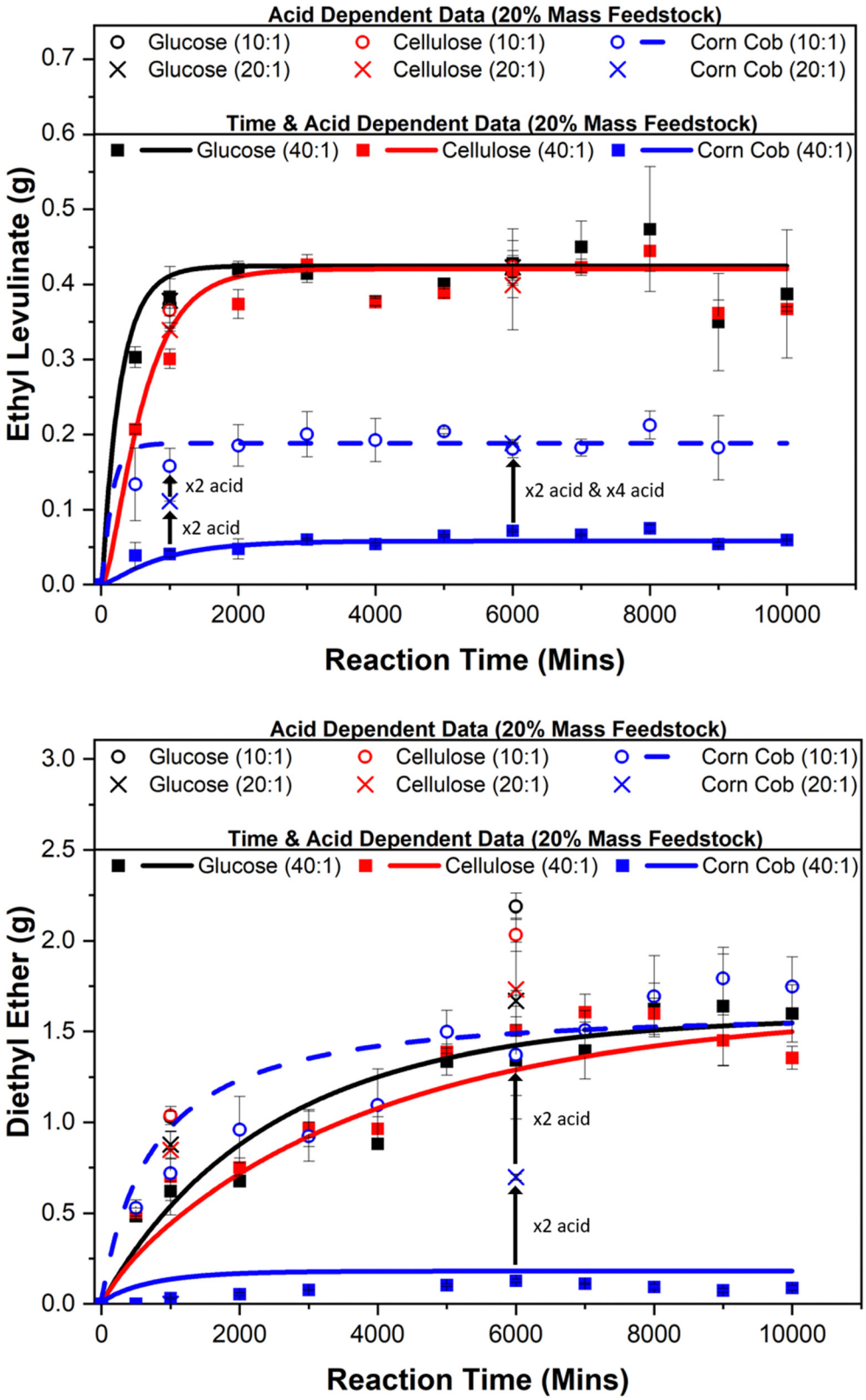

Fig. 5 Ethyl levulinate (g) and diethyl ether (g) produced from the sulphuric acid-catalysed ethanolysis of glucose, cellulose, and corn cob (5, 10, and 20 mass percent) for three different feedstock-to-acid ratios (10 : 1, 20 : 1, and 40 : 1) at 150 °C. Full time-dependent data sets are produced for a feedstock-to-acid ratio of 40. An additional time-dependent data set was produced for corn cob only at a feedstock-to-acid ratio of 10 : 1. At 1000 and 6000 minutes, reactions are performed varying the feedstock-to-acid ratio (10 : 1, 20 : 1, and 40 : 1) to determine the acid dependence of the process in both the kinetic and steady-state phases. The square, cross, and circle data points represent experimental data, and the lines represent the chemical kinetic model.

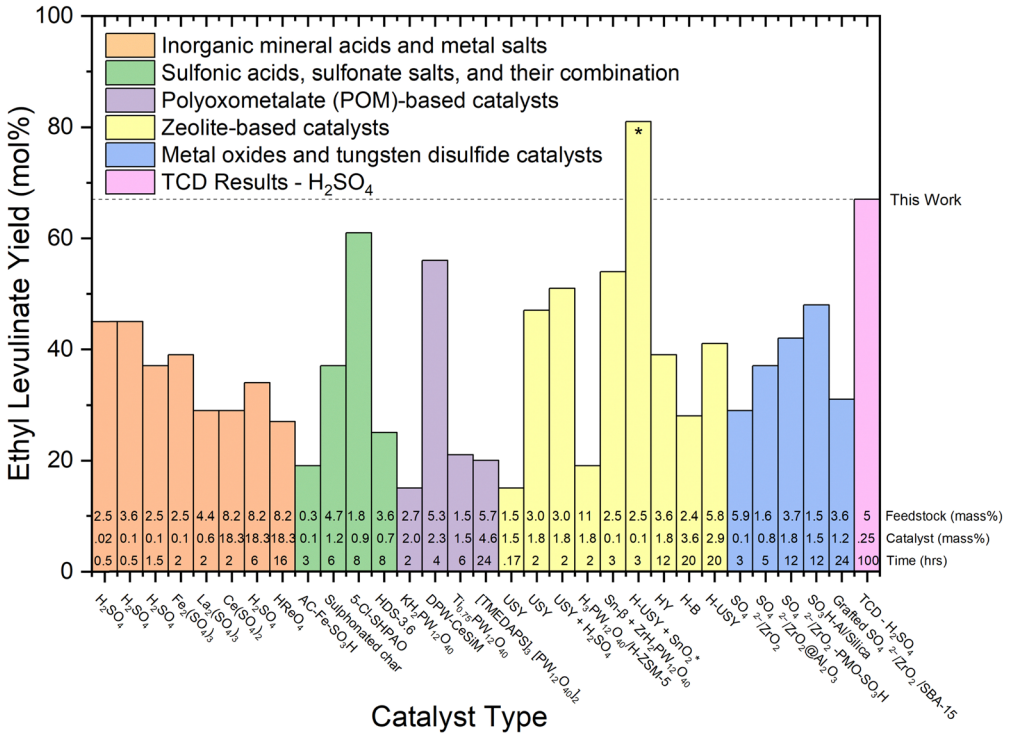

Fig. 7 Literature review of experimental yields of ethyl levulinate using various catalyst types.[17,18,21,22,27,29,30,32,37–39,41–43,47,50,51,53,60,67–71] All reaction systems use conventional heating and a one-pot process, excluding the H-USY-SnO_2 marked with a "*" symbol, which integrates heating and spinning. The feedstock loading (mass%), catalyst loading (mass%), and reaction times are displayed at the bottom of each column.

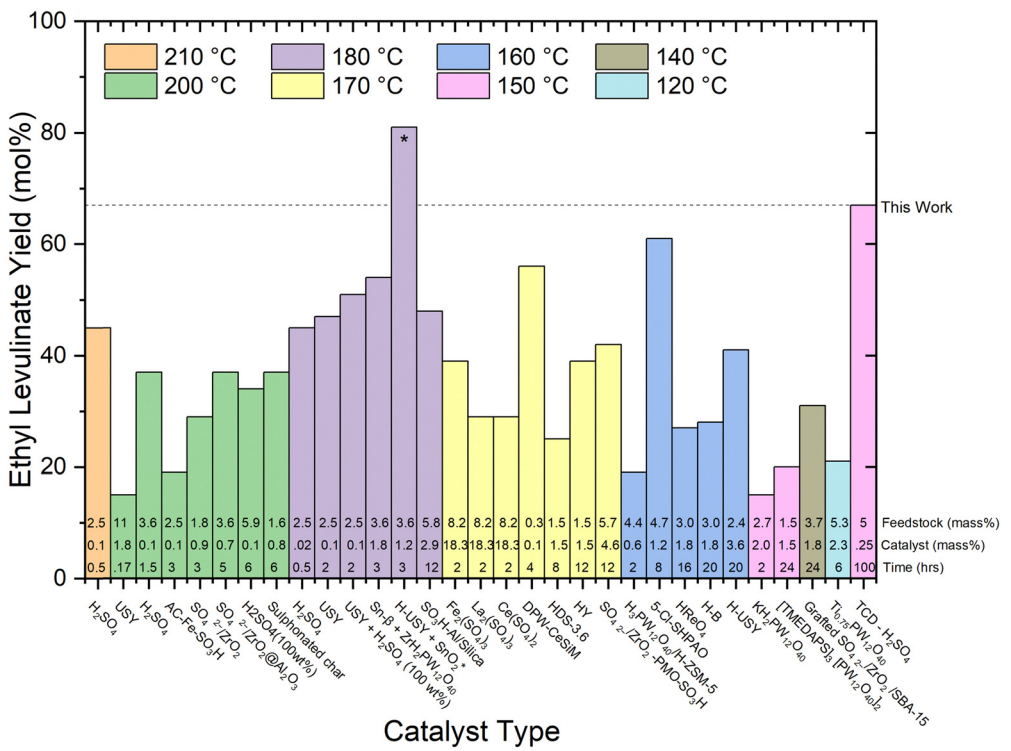

Fig. 8 Literature review of experimental yields of ethyl levulinate using various catalyst types.[17,18,21,22,27,29,30,32,37–39,41–43,47,50,51,53,60,67–71] All reaction systems use conventional heating and a one-pot process, excluding the H-USY-SnO_2 marked with a "*" symbol, which integrates heating and spinning. The feedstock loading (mass%), catalyst loading (mass%), and reaction times are displayed at the bottom of each column.

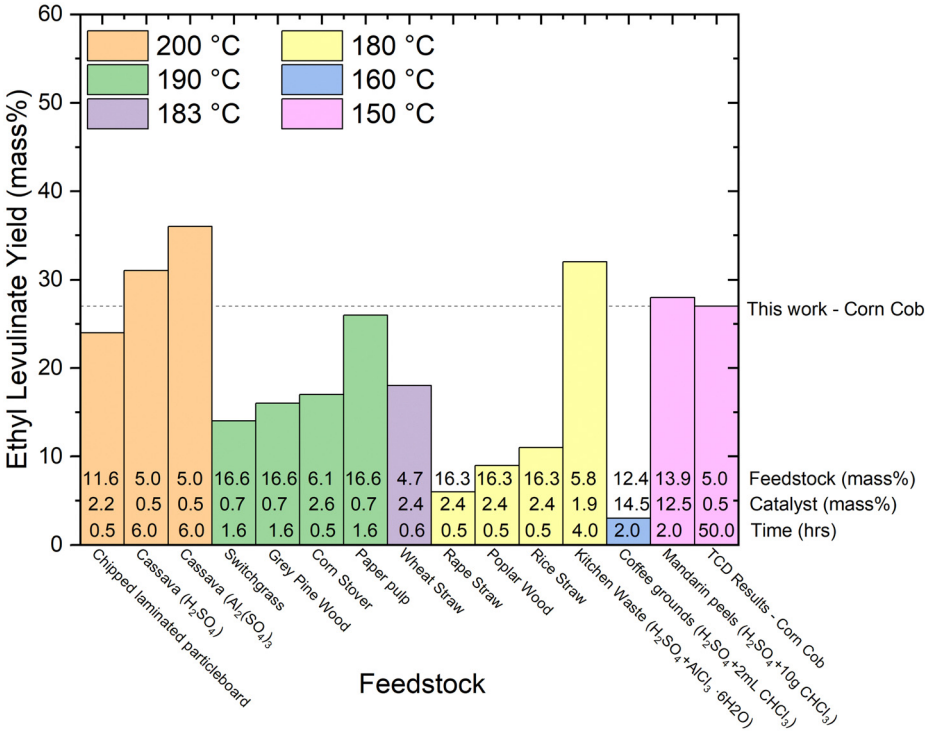

Fig. 9 Literature review of experimental yields of ethyl levulinate categorized by temperature from various real biomasses.[72–80] The feedstock loading (mass%), catalyst loading (mass%), and reaction times are displayed at the bottom of each column. All reactions are a one-pot process and use sulphuric acid as the catalyst unless otherwise stated.

5.4. Comparison with literature

Numerous studies have detailed the acid-catalysed hydrolysis of carbohydrates in other alcohols in a one-pot system. These reports were recently addressed in a comprehensive review by Galletti and co-workers.[6]

Fig. 7–9 analyse the ''yield'' of ethyl levulinate reported by literature studies as a function of (i) catalyst type, (ii) reaction temperature, and (iii) feedstock type, respectively. Fig. 7 and 8 only consider glucose as the feedstock, and thus, all yields have been converted to molar yields based on eqn (1). Fig. 9 compares real-world biomass, and therefore, all yields are converted to mass yields, consistent with all yields reported in this work.

On examination of the literature in this way, it is clear that there has been no coherent overarching attempt to systematically study the reaction conditions with a view to understanding their influence on the rate and/or yield of ethyl levulinate. Rather, the studies are more of a stand-alone nature, resulting in an unorganised ensemble of experimental parameters and associated observations. This sort of ensemble may lend itself to mathematical analysis such as multiple linear regression, or principal component analysis, whereby the dependence of a performance variable (ethyl levulinate concentration) is delineated with respect to each parameter of an ensemble. In this example, the ensemble would be catalyst type, catalyst concentration, reaction temperature, feedstock type, feedstock concentration, and importantly, reaction time. Efforts to form an accurate multiple linear regression model for this literature data produced a low-quality model. This is due to the variability in experimental parameters being too wide, and insufficient experimental data. The model is provided as ESI.†

Though an entirely objective numerical assessment of the importance of each parameter is, at the moment, inconclusive, even with the wide variability in conditions studied, given the data available, we believe that the following basic statements are essentially true.

1. Longer reaction times achieve higher ethyl levulinate ''yields'', until the steady state of ethyl levulinate production has been achieved.

2. Higher reaction temperatures achieve higher ethyl levulinate ''yields'', but do not affect the ethyl levulinate ''yield'' once steady state has been achieved.

3. Higher feedstock loadings achieve lower ethyl levulinate ''yields''.

4. Reaction time, reaction temperature, and feedstock loading appear to be dominant determinators of ''yield''.

5. There appears to be no clearly discernible influence on the effectiveness of particular catalysts to achieve greater actual steady state yields. From Fig. 7, of the five generic classes of catalyst, comparably high yields of 56, 61, 67, and 81 mol% are achieved with four different catalyst types, notably also dependent on reaction time and temperature. Reports of the performance of the zeolite catalyst class indicate they may produce a marginally higher yield of ethyl levulinate, but this is not at all conclusive.

6. With regard to feedstock identity, yields obtained with actual biomasses are significantly lower than those achieved with glucose or cellulose. The higher yields are reported for

corn cob (27%, this study), Mandarin peel (28%), and Cassava (31 and 36%). Given our understanding that the alkyl levulinates are principally produced from the cellulosic fraction of the biomass, these observations are plausible. It is important to note that nine of the thirteen studies on real biomasses, report yields much lower than 25%.

5.5. Ether effect: composition of reaction mixtures

Despite the surge of interest in the synthesis of alkyl levulinates from pure carbohydrates and lignocellulosic biomass, studies rarely determine the concentrations of the other main co-product, dialkyl ether, and the other feedstock, the alcohol.[18,21,75,76,81,82] In literature studies, optimal yields of ethyl levulinate are targeted without consideration of the formation of major co-products, knowledge of which is essential to determining techno-economics. This trend tends to result in the studies configuring a lower feedstock concentration relative to the ethanol and acid concentrations so as to achieve maximum yields of ethyl levulinate. It is important to appreciate the difference between the yield of product (a ratio) and quantity of product (how much is produced in unit batch). Additionally, this practice has the unintended and undesirable effect of maximising the production of dialkyl ether. Surprisingly, the ether effect appears to be mostly overlooked in the literature.

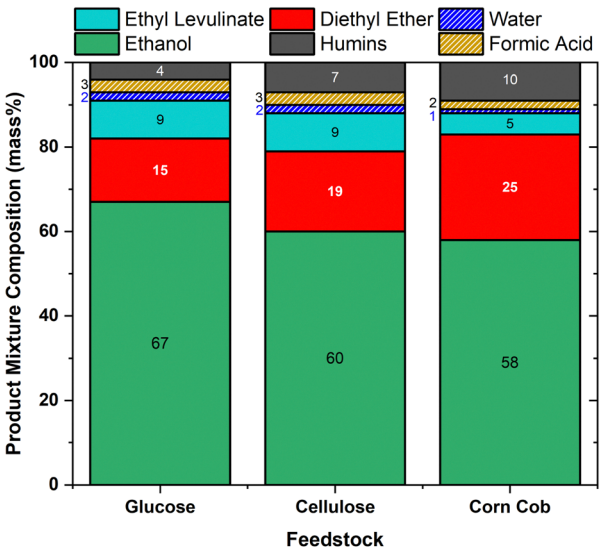

Fig. 10 Composition of the reaction mixture (mass%) at reaction conditions that give the highest ethyl levulinate to diethyl ether ratio normalised to 100% based on the 6 main components of the reaction mixtures. The ethyl levulinate, diethyl ether, ethanol, and humins concentrations are experimentally measured. The water and formic acid concentrations are calculated stoichiometrically.

Table 5 Coefficient of determination (R^2) and fidelity index of glucose, cellulose, and corncob

	Error (R^2)			
Feedstock	Ethyl levulinate	Diethyl ether	Ethanol	Fidelity index (%)
Glucose	0.97	0.94	0.97	86.1
Cellulose	0.97	0.94	0.97	85.2
Corncob	0.87	0.95	0.97	84.5

Fig. 10 shows the product concentrations (mass%) at the shortest time at which the steady state of ethyl levulinate production has been reached, for 20 mass% of feedstock (with 1 mass% sulphuric acid for glucose and cellulose and 2 mass% sulphuric acid for corn cob), as this produced the highest concentration of ethyl levulinate relative to diethyl ether out of the three feedstock loadings. The concentrations of ethyl levulinate, diethyl ether, ethanol, and humins are experimentally determined as above, whereas the content of water and formic acid are modelled stoichiometrically from eqn (1)–(4).

For cellulose and glucose, Fig. 10 shows that ethyl levulinate represents 9 mass% of the reaction mixture for both feedstocks,

Table 4 Elucidated kinetic model. rate constants, k, determined at 150 °C

#	Reaction	k ($cm^3\ mol^{-1}\ s^{-1}$)
1	$C_2H_5OH + H^+ \rightleftharpoons C_2H_5OH_2^+$	2.34×10^{10}
2	$H_2O + H^+ \rightleftharpoons H_3O^+$	3.74×10^{8}
3	$C_2H_5OH + C_2H_5OH_2^+ \rightleftharpoons C_2H_5OC_2H_5 + H_3O^+$	1.34×10^{4}
4	$C_6H_{12}O_6 + C_2H_5OH_2^+ \rightarrow C_8H_{16}O_6 + H_3O^+$	5.20×10^{5}
5	$C_8H_{16}O_6 + C_2H_5OH_2^+ \rightarrow C_7H_{12}O_3 + HCOOH + H_2O + C_2H_5OH_2^+$	8.26×10^{6}
6	$C_6H_{12}O_6 + H^+ \rightarrow Unknown(H^+)_{Glucose} + 3.5H_2O$	2.37×10^{5}
7	$C_6H_{12}O_6 + H^+ \rightarrow Unknown_{Glucose} + 3H_2O + H^+$	1.03×10^{1}
8	$C_8H_{16}O_6 + H^+ \rightarrow Unknown(H^+)_{Ethylglucoside} + 4.5H_2O$	5.45×10^{-1}
9	$C_8H_{16}O_6 + H^+ \rightarrow Unknown_{Ethylglucoside} + 4H_2O + H^+$	1.19×10^{2}
10	$(C_6H_{10}O_5)_n + H_3O^+ \rightarrow C_6H_{12}O_6 + H^+$	2.00×10^{7}
11	$(C_6H_{10}O_5)_n + C_2H_5OH_2^+ \rightarrow C_8H_{16}O_6 + H^+$	4.48×10^{5}
12	$(C_6H_{10}O_5)_n + H^+ \rightarrow Unknown(H^+)_{Cellulose} + 2.5H_2O$	8.84×10^{0}
13	$(C_6H_{10}O_5)_n + H^+ \rightarrow Unknown_{Cellulose} + 2H_2O + H^+$	2.57×10^{1}
14	$Corn\ cob + H^+ \rightarrow 0.882\ (C_5H_8O_4)_n + (C_6H_{10}O_5)_n + Lignin + H^+$	1.00×10^{11}
15	$Lignin + H^+ \rightarrow Unknown(H^+)_{Lignin}$	1.41×10^{1}
16	$Lignin + H^+ \rightarrow Unknown_{Lignin} + H^+$	7.31×10^{0}
17	$Hemicellulose + H^+ \rightarrow Unknown(H^+)_{Hemicellulose} + 2H_2O$	9.98×10^{2}
18	$Hemicellulose + H^+ \rightarrow Unknown_{Hemicellulose} + H^+ + 1.5H_2O$	7.11×10^{3}

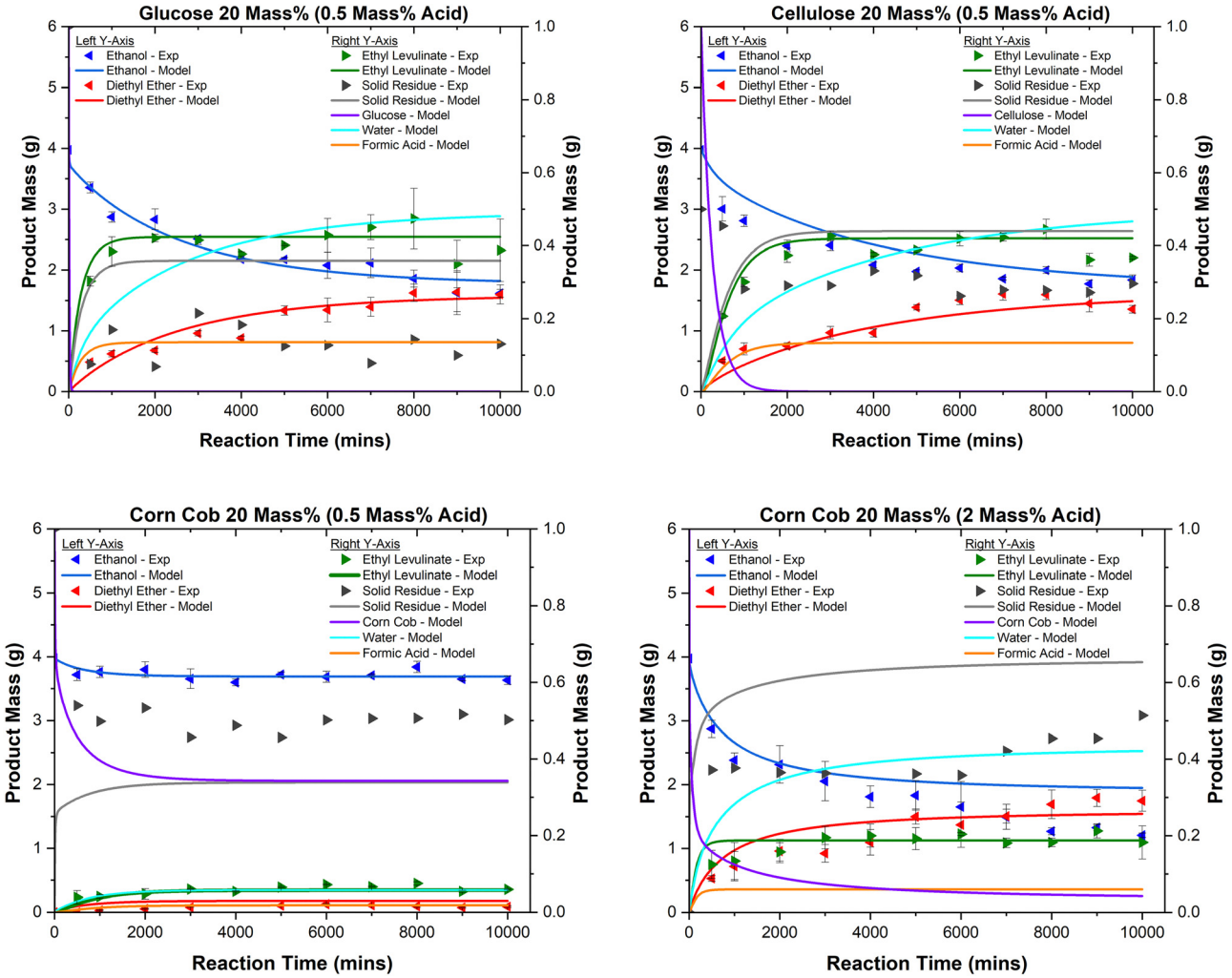

Fig. 11 Product concentrations as a function of time for the acid-catalysed (0.5 mass%) ethanolysis of glucose (top left), cellulose (top right), corn cob (bottom left) and corn cob with 2 mass% of sulphuric acid (bottom right) at 20 mass% of feedstock at 150 °C. All data points shown are the average of four experimentally determined data points, while the error bars are the standard deviation of those four points. All lines are produced by the chemical kinetic model where "Solid Residue – Model" is calculated by summing the masses of all species labelled as "unknown" in Fig. 3 and Table 4.

with ether at 15 and 19 mass%, respectively. Conversely, for the real-world biomass, corn cob, ethyl levulinate is 5 mass%. Not surprisingly, the latter feedstock produced more diethyl ether as the amount of acid added is the highest. Therefore, to minimize the diethyl production while maximising ethyl levulinate formation, a minimum concentration of sulphuric acid should be used. Results show that this ideal feedstock : acid ratio falls in the range 10 : 1–20 : 1 at 150 °C for corn cob.

From Fig. 9, the catalyst concentrations typically employed in the literature are large, in the order of 0.5–15 mass%. Given that the analysis of Fig. 10 uses a lower concentration, 0.5–2% acid, it is reasonable to assume that the use of higher acid fractions would result in higher ether concentrations. Likewise, from Fig. 9, the feedstock concentrations employed in this study are higher than that of most literature. This means that in available studies, ether formation is higher than what is depicted in Fig. 10. Alcohol consumption and ether formation significantly affect the techno-economic viability of the process, which underscores the need for a fundamental knowledge of the ether effects.

5.6. Chemical kinetic model

Currently, the reaction pathways and kinetics of the acid-catalysed ethanolysis of lignocellulosic biomass are not fundamentally known. The model is evaluated against the time-resolved experimental data to derive the empirical rate constants associated with each reaction in the model reaction network. Three consecutive optimisations of the glucose, cellulose, and corncob sub-models against each set of feedstock experimental data resulted in the kinetic rate constants listed in Table 4. The validity of the model in calculating the mass of ethyl levulinate and diethyl ether produced is assessed by a fidelity index for each of the feedstocks employed.

The R^2 value of the model for ethyl levulinate production from glucose, cellulose, and corncob are 0.97, 0.97, and 0.87, respectively, as displayed in Table 5. It should be stressed that

both R^2 and the fidelity index measure the capability of the model in predicting the behaviour of glucose, cellulose, and corncob under ethanolysis conditions. The difference in the rate of formation of ethyl levulinate between glucose and cellulose is reproduced by the model with the reaction rate constant of the depolymerisation reactions of cellulose, reactions (10) and (11). The corncob surrogate model species, which consists of a non-interacting mixture of cellulose, hemicellulose, and lignin, only considers a reaction pathway to ethyl levulinate from cellulose. This simplified picture accurately predicted the yield reduction in the corncob ethanolysis. The R^2 value of the model for diethyl ether production from glucose, cellulose, and corncob are 0.94, 0.94, and 0.95, respectively. The mass of diethyl ether decreases with increasing mass loading. This is due to the lower initial mass of ethanol in the system and the ''unknowns'' formation through non-catalytic reactions. Notably, the model captures these effects. There is a higher rate of formation of diethyl ether in the glucose model, compared to that of cellulose, as a result of the acid consumption in the reaction of cellulose to ''Unknowns''. Under similar conditions, the mass of diethyl ether formed is significantly less for corn cob than for glucose and cellulose, which the model also replicates. In these reactions, hemicellulose and lignin react with a proton to produce ''Unknowns'', reducing the population of the latter and hindering the formation of diethyl ether.

Fig. 3 summarises the elucidated kinetic model, which consists of 18 elementary steps. It should be emphasised that reactions (3)–(9) are optimised to all glucose data. Reactions (10)–(13) are optimised to cellulose data. Reactions (15)–(18) are optimised to corncob data. The composition of ''unknown'' variables is contingent upon the source species and the catalytic nature of the reaction under consideration.

Fig. 11 shows the species concentration as a function of time for the sulphuric acid-catalysed ethanolysis of glucose, cellulose, and corn cob (20 mass%) at 150 °C as produced by the model. The model accurately predicts the relationship between these variables, overestimating, however, the mass of solid residue. This inconsistency might be related to the soluble species of humins present in the reaction mixture. This may also be due to the mass loss of humins during centrifugation, which is highlighted in the elemental balance results section. Moreover, the effect of reactant concentration and the extent of hydrogen cation consumption on the relative concentrations of ethyl levulinate, diethyl ether, and ethanol are accurately reproduced by the model.

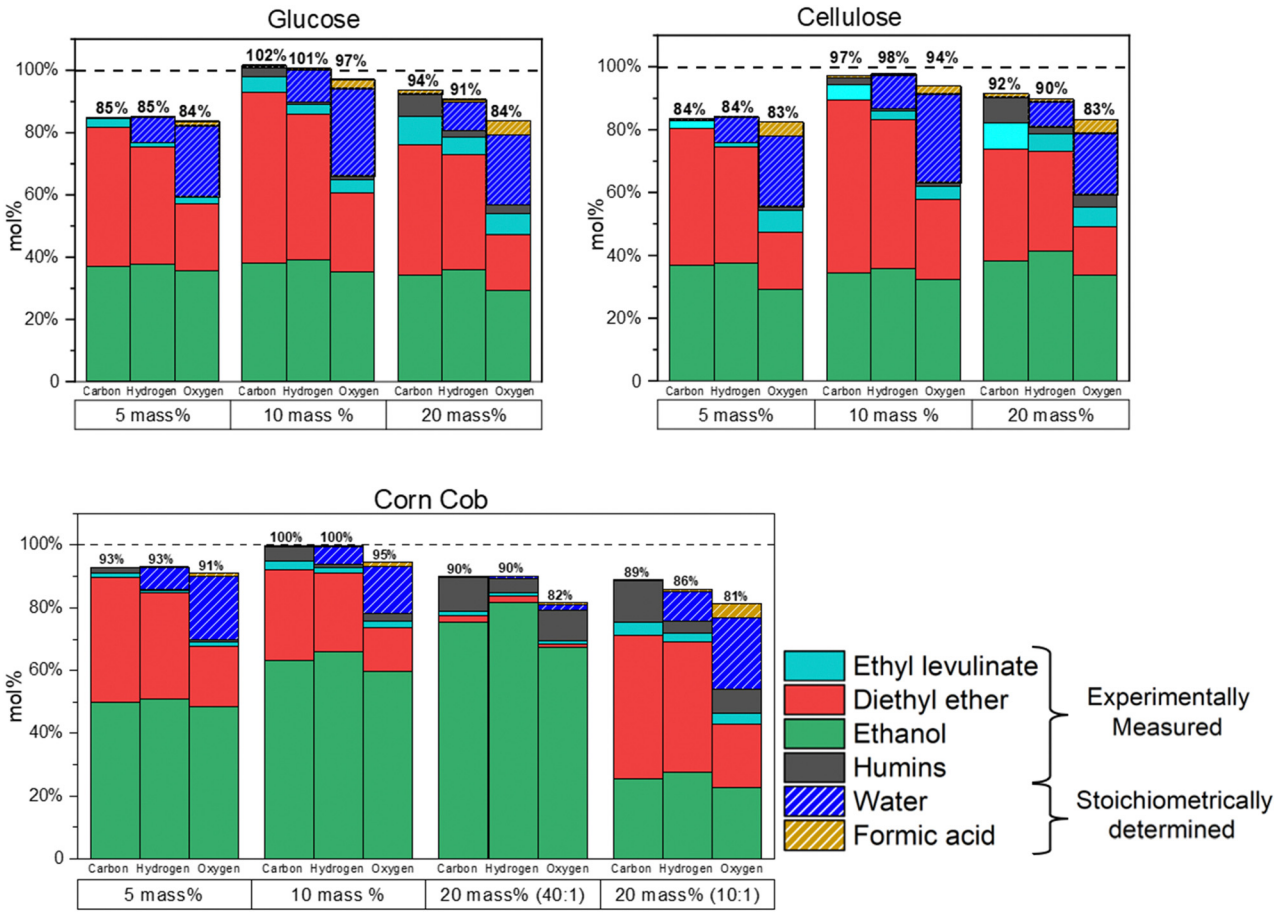

Fig. 12 Mol% of carbon, hydrogen, and oxygen recovered at the end of 5, 10, 20 mass% glucose, cellulose, and corn cob ethanolysis for 10 000 minutes at 150 °C.

5.7. Elemental balance

An elemental balance is performed to aid in the TEA of the process. The moles of carbon, hydrogen, and oxygen in the products of this reaction (ethyl levulinate, diethyl ether, ethanol, humins, formic acid, and water) are quantified and expressed as a percentage of the moles of carbon, hydrogen, and oxygen present in both the feedstock and added ethanol. The concentrations of ethyl levulinate, diethyl ether, and ethanol are determined *via* gas chromatography. Two principal sources of potential mass loss are identified in the process: (i) loss of gases and (ii) humins loss during centrifugation. Both mechanisms are responsible for the trends observed in Fig. 12. Mass loss is greatest in both the 5 and 20 mass% of feedstock reactions.

For 5 mass% of feedstock, there are higher ethanol and acid concentrations relative to feedstock. This favours the formation of diethyl ether and thus increases the pressure inside the reactor. Higher pressures resulted in a greater mass loss during the reaction. In contrast, for 20 mass% of feedstock, a higher humins formation is observed, and thus the loss increases during centrifugation.

6. Conclusions

A self-consistent, hierarchical, and mass-conserved chemical kinetic model that accurately replicates experiments of the ethanolysis of glucose, cellulose, and corncob is elucidated and validated. As a key novelty, the model employs the biochemical composition of the corn cob as a compositional surrogate, extending fundamental orientated kinetic modelling to actual biomasses, opening the door to allow kinetic models inform more comprehensive techno-economic-analyses of lignocellulose ethanolysis to produce advanced biofuels. To construct the model, a complete and high-quality experimental dataset for the steady state conditions of ethyl levulinate production *via* sulphuric acid-catalysed ethanolysis at 150 °C for 5, 10, and 20 mass% for glucose, cellulose, and corn cob is established.

At all steady state conditions, diethyl ether is observed as the major reaction product. Minimum diethyl ether concentrations relative to ethyl levulinate are achieved at the highest feedstock loading (20 mass%), resulting in mass ratios of approximately 2 : 1, 2 : 1, and 5 : 1, for glucose, cellulose, and corn cob, respectively. The critical corn cob-to-acid mass ratio that minimizes the formation of undesired co-products (diethyl ether) ranged from 10–20 : 1 at 150 °C. The concentration of ethyl levulinate at steady state, and the time needed to reach steady state is specifically targeted as it is key information for techno-economic-analyses (TEA). The required time to reach the steady state at 150 °C is found to be dependent on the relative complexity of each feedstock in the order of glucose (1000 minutes), cellulose (2000 minutes), and corn cob (3000 minutes). It is shown that the maximum average steady state yields (mass%) of ethyl levulinate from glucose, cellulose, and corn cob are respectively, (46.6 ± 3.7), (50.2 ± 5.4) and (27.0 ± 1.9)% and are achieved at 5 mass% feedstock, 0.5 mass% sulphuric acid, and 94.5 mass% ethanol.

Surprisingly, analysis shows that the yield of ethyl levulinate achieved from corn cob is higher than that predicted based on the cellulose content of the corn cob, and the experimentally determined ethyl levulinate yields from pure cellulose, therefore implying alternative sources of ethyl levulinate formation. This discovery indicates ethyl levulinate may be formed by atypical conversions of the other biochemical constituents of corn cob, such as hemicellulose, directly challenging the common assumption that all ethyl levulinate produced from lignocellulosic biomass comes from its cellulose content alone.

Furthermore, as expected, the steady state concentration of ethyl levulinate formed from glucose and cellulose is found to be independent of the acid concentration. Therefore, the conversion of glucose and cellulose to ethyl levulinate in the presence of ethanol and sulphuric acid is concluded to be truly catalytic in nature. Conversely, in the case of corn cob, the steady state concentration of ethyl levulinate is shown to be highly dependent on the acid concentration until a maximum quantity of ethyl levulinate is achieved. The observations presented are consistent with a basic hypothesis that the hydrogen cations originating from the acid catalyst are consumed in some irreversible process. This is further evidenced by the negligible quantities of diethyl ether observed for experiments using the lowest corn cob-to-acid mass ratio (40 : 1), indicating that the ethanolysis of lignocellulosic biomass is not wholly a catalytic process.

Abbreviations

RED	Renewable energy directive
RFS	Renewable fuel standard
EU	European union
HMF	Hydroxymethyl furfural
EMF	Ethoxymethyl furfural
EL	Ethyl levulinate
DEE	Diethyl ether
EtOH	Ethanol
Humins	Solid residue left after reaction
TEA	Techno-economic-analysis
PES	Potential energy surface
LA	Levulinic acid
DMSO	Dimethyl sulfoxide

Conflicts of interest

There are no conflicts to declare.

Acknowledgements

This publication has emanated from research conducted with the financial support of Science Foundation Ireland [20/EPSRC/3701] and the Engineering and Physical Sciences Research Council [EP/T033088/1]. This project is also co-funded by the

Ryanair Sustainable Aviation Research Centre at Trinity College Dublin, the European Union, through the European Research Council, Mod-L-T, action number 101002649.

References

1 IEA, Tracking Transport 2020, IEA, Paris, 2020, **https://www.iea.org/reports/tracking-transport-2020**.
2 Directive (EU) 2018/2001 of the European Parliament and of the Council of 11 December 2018 on the promotion of the use of energy from renewable sources, 2018.
3 Y.-K. Oh, K.-R. Hwang, C. Kim, J. R. Kim and J.-S. Lee, Recent developments and key barriers to advanced biofuels: A short review, *Bioresour. Technol.*, 2018, **257**, 320–333.
4 J. Witcover and R. B. Williams, Comparison of ''Advanced'' biofuel cost estimates: trends during rollout of low carbon fuel policies, *Trans. Res., Part D: Trans. Environ.*, 2020, **79**, 102211.
5 Y. Sun and J. Cheng, Hydrolysis of lignocellulosic materials for ethanol production: a review, *Bioresour. Technol.*, 2002, **83**, 1–11.
6 A. M. Raspolli Galletti, C. Antonetti, S. Fulignati and D. Licursi, Direct Alcoholysis of Carbohydrate Precursors and Real Cellulosic Biomasses to Alkyl Levulinates: A Critical Review, *Catalysts*, 2020, **10**, 1221.
7 F.-X. Collard and J. Blin, A review on pyrolysis of biomass constituents: mechanisms and composition of the products obtained from the conversion of cellulose, hemicelluloses and lignin, *Renewable Sustainable Energy Rev.*, 2014, **38**, 594–608.
8 A. Molino, V. Larocca, S. Chianese and D. Musmarra, Biofuels Production by Biomass Gasification: A Review, *Energies*, 2018, **11**, 811.
9 J. A. Ramirez, R. J. Brown and T. J. Rainey, A Review of Hydrothermal Liquefaction Bio-Crude Properties and Prospects for Upgrading to Transportation Fuels, *Energies*, 2015, **8**, 6765–6794.
10 T. Wang, Y. Zhai, Y. Zhu, C. Li and G. Zeng, A review of the hydrothermal carbonization of biomass waste for hydrochar formation: process conditions, fundamentals, and physicochemical properties, *Renewable Sustainable Energy Rev.*, 2018, **90**, 223–247.
11 E. Christensen, A. Williams, S. Paul, S. Burton and R. L. McCormick, Properties and performance of levulinate esters as diesel blend components, *Energy Fuels*, 2011, **25**, 5422–5428.
12 K. C. Badgujar, V. C. Badgujar and B. M. Bhanage, A review on catalytic synthesis of energy rich fuel additive levulinate compounds from biomass derived levulinic acid, *Fuel Process. Technol.*, 2020, **197**, 106213.
13 A. Démolis, N. Essayem and F. Rataboul, Synthesis and Applications of Alkyl Levulinates, *ACS Sustainable Chem. Eng.*, 2014, **2**, 1338–1352.
14 T. Flannelly, S. Dooley and J. J. Leahy, Reaction Pathway Analysis of Ethyl Levulinate and 5-Ethoxymethylfurfural from D-Fructose Acid Hydrolysis in Ethanol, *Energy Fuels*, 2015, **29**, 7554–7565.
15 M. S. Howard, G. Issayev, N. Naser, S. M. Sarathy, A. Farooq and S. Dooley, Ethanolic gasoline, a lignocellulosic advanced biofuel, Sustainable, *Energy Fuels*, 2019, **3**, 409–421.
16 J. F. Leal Silva, R. Grekin, A. P. Mariano and R. Maciel, Filho, Making Levulinic Acid and Ethyl Levulinate Economically Viable: A Worldwide Technoeconomic and Environmental Assessment of Possible Routes, *Energy Technol.*, 2018, **6**, 613–639.
17 J. R. Bernardo, M. C. Oliveira and A. C. Fernandes, HReO4 as highly efficient and selective catalyst for the conversion of carbohydrates into value added chemicals, *Mol. Catal.*, 2019, **465**, 87–94.
18 M. Bosilj, J. Schmidt, A. Fischer and R. J. White, One pot conversion of glucose to ethyl levulinate over a porous hydrothermal acid catalyst in green solvents, *RSC Adv.*, 2019, **9**, 20341–20344.
19 C. Ming, K. Sun, Y. Shao, Z. Zhang, S. Zhang, Q. Liu, Y. Wang, S. Hu, J. Xiang and X. Hu, Conversion of Cellulose to Levulinic Acid/Ester over an Acid Catalyst: Impacts of Dispersion of Hydrogen Ions on Polymerization Reactions, *Energy Fuels*, 2019, **33**, 11187–11199.
20 G. Xu, C. Chang, S. Fang and X. Ma, Cellulose reactivity in ethanol at elevate temperature and the kinetics of one-pot preparation of ethyl levulinate from cellulose, *Renewable Energy*, 2015, **78**, 583–589.
21 G. Xu, B. Chen, Z. Zheng, K. Li and H. Tao, One-pot ethanolysis of carbohydrates to promising biofuels: 5-ethoxymethylfurfural and ethyl levulinate, *Asia-Pac. J. Chem. Eng.*, 2017, **12**, 527–535.
22 G.-Z. Xu, C. Chang, W.-N. Zhu, B. Li, X.-J. Ma and F.-G. Du, A comparative study on direct production of ethyl levulinate from glucose in ethanol media catalysed by different acid catalysts, *Chem. Pap.*, 2013, **67**, 1355–1363.
23 Y.-B. Huang, T. Yang, Y.-T. Lin, Y.-Z. Zhu, L.-C. Li and H. Pan, Facile and high-yield synthesis of methyl levulinate from cellulose, *Green Chem.*, 2018, **20**, 1323–1334.
24 R. Liu, J. Chen, X. Huang, L. Chen, L. Ma and X. Li, Conversion of fructose into 5-hydroxymethylfurfural and alkyl levulinates catalyzed by sulfonic acid-functionalized carbon materials, *Green Chem.*, 2013, **15**, 2895–2903.
25 K. Sun, L. Zhang, Y. Shao, Q. Li, H. Fan, G. Gao, S. Zhang, Q. Liu, Y. Wang and X. Hu, Conversion of monosaccharides into levulinic acid/esters: impacts of metal sulfate addition and the reaction medium, *J. Chem. Technol. Biotechnol.*, 2019, **94**, 3676–3686.
26 L. Zhou, D. Gao, J. Yang, X. Yang, Y. Su and T. Lu, Conversion of recalcitrant cellulose to alkyl levulinates and levulinic acid via oxidation pretreatment combined with alcoholysis over $Al_2(SO_4)_3$, *Cellulose*, 2020, **27**, 1451–1463.
27 J. Gu, J. Zhang, D. Li, H. Yuan and Y. Chen, Hyper-crosslinked polymer based carbonaceous materials as efficient catalysts for ethyl levulinate production from carbohydrates, *J. Chem. Technol. Biotechnol.*, 2019, **94**, 3073–3083.

28 S. Karnjanakom, P. Maneechakr, C. Samart, S. Kongparakul, G. Guan and A. Bayu, Direct conversion of sugar into ethyl levulinate catalyzed by selective heterogeneous acid under co-solvent system, *Catal. Commun.*, 2020, **143**, 106058.
29 F. Yu, R. Zhong, H. Chong, M. Smet, W. Dehaen and B. F. Sels, Fast catalytic conversion of recalcitrant cellulose into alkyl levulinates and levulinic acid in the presence of soluble and recoverable sulfonated hyperbranched poly(arylene oxindole)s, *Green Chem.*, 2017, **19**, 153–163.
30 J. Zhang and J. Chen, Modified solid acids derived from biomass based cellulose for one-step conversion of carbohydrates into ethyl levulinate, *J. Energy Chem.*, 2016, **25**, 747–753.
31 L. Zhang, Y. Zhu, L. Tian, Y. He, H. Wang and F. Deng, One-pot alcoholysis of carbohydrates to biofuel 5-ethoxymethylfufural and 5-methoxymethylfufural via a sulfonic porous polymer, *Fuel Process. Technol.*, 2019, **193**, 39–47.
32 J. Chen, G. Zhao and L. Chen, Efficient production of 5-hydroxymethylfurfural and alkyl levulinate from biomass carbohydrate using ionic liquid-based polyoxometalate salts, *RSC Adv.*, 2014, **4**, 4194–4202.
33 W. Deng, M. Liu, Q. Zhang and Y. Wang, Direct transformation of cellulose into methyl and ethyl glucosides in methanol and ethanol media catalyzed by heteropolyacids, *Catal. Today*, 2011, **164**, 461–466.
34 D. Gupta, C. Mukesh and K. K. Pant, Topotactic transformation of homogeneous phosphotungastomolybdic acid materials to heterogeneous solid acid catalyst for carbohydrate conversion to alkyl methylfurfural and alkyl levulinate, *RSC Adv.*, 2020, **10**, 705–718.
35 P. F. Pinheiro, D. M. Chaves and M. J. da Silva, One-pot synthesis of alkyl levulinates from biomass derivative carbohydrates in tin(II) exchanged silicotungstates-catalyzed reactions, *Cellulose*, 2019, **26**, 7953–7969.
36 C. Song, S. Liu, X. Peng, J. Long, W. Lou and X. Li, Catalytic Conversion of Carbohydrates to Levulinate Ester over Heteropolyanion-Based Ionic Liquids, *ChemSusChem*, 2016, **9**, 3307–3316.
37 S. Zhao, G. Xu, C. Chang, S. Fang, Z. Liu and F. Du, Direct Conversion of Carbohydrates into Ethyl Levulinate with Potassium Phosphotungstate as an Efficient Catalyst, *Catalysts*, 2015, **5**, 1897–1910.
38 S. B. Rao, K. P. Kumari, D. D. Lakshmi and N. Lingaiah, One pot selective transformation of biomass derived chemicals towards alkyl levulinates over titanium exchanged heteropoly tungstate catalysts, *Catal. Today*, 2018, **309**, 269–275.
39 C. Chang, G. Xu, W. Zhu, J. Bai and S. Fang, One-pot production of a liquid biofuel candidate—Ethyl levulinate from glucose and furfural residues using a combination of extremely low sulfuric acid and zeolite USY, *Fuel*, 2015, **140**, 365–370.
40 H. Li, Z. Fang and S. Yang, Direct Conversion of Sugars and Ethyl Levulinate into γ-Valerolactone with Superparamagnetic Acid–Base Bifunctional $ZrFeO_x$ Nanocatalysts, *ACS Sustainable Chem. Eng.*, 2016, **4**, 236–246.
41 N. Mulik, P. Niphadkar and V. Bokade, Synergetic combination of $H_2Zr_1PW_{12}O_{40}$ and Sn-Beta as potential solid acid catalyst for direct one-step transformation of glucose to ethyl levulinate, a biofuel additive, *Environ. Progress Sustainable Energy*, 2019, **38**, 13173.
42 S. Saravanamurugan and A. Riisager, Zeolite Catalyzed Transformation of Carbohydrates to Alkyl Levulinates, *ChemCatChem*, 2013, **5**, 1754–1757.
43 D. Song, Q. Zhang, Y. Sun, P. Zhang, Y.-H. Guo and J.-L. Hu, Design of Ordered Mesoporous Sulfonic Acid Functionalized ZrO2/organosilica Bifunctional Catalysts for Direct Catalytic Conversion of Glucose to Ethyl Levulinate, *ChemCatChem*, 2018, **10**, 4953–4965.
44 A. S. Amarasekara and B. Wiredu, Acidic Ionic Liquid Catalyzed One-Pot Conversion of Cellulose to Ethyl Levulinate and Levulinic Acid in Ethanol-Water Solvent System, *BioEnergy Res.*, 2014, **7**, 1237–1243.
45 S. Saravanamurugan, O. Nguyen Van Buu and A. Riisager, Conversion of Mono- and Disaccharides to Ethyl Levulinate and Ethyl Pyranoside with Sulfonic Acid-Functionalized Ionic Liquids, *ChemSusChem*, 2011, **4**, 723–726.
46 Z. Babaei, A. Najafi Chermahini and M. Dinari, Alumina-coated mesoporous silica SBA-15 as a solid catalyst for catalytic conversion of fructose into liquid biofuel candidate ethyl levulinate, *Chem. Eng. J.*, 2018, **352**, 45–52.
47 J. Heda, P. Niphadkar and V. Bokade, Efficient Synergetic Combination of H-USY and SnO_2 for Direct Conversion of Glucose into Ethyl Levulinate (Biofuel Additive), *Energy Fuels*, 2019, **33**, 2319–2327.
48 E. Y. C. Jorge, C. G. S. Lima, T. M. Lima, L. Marchini, M. B. Gawande, O. Tomanec, R. S. Varma and M. W. Paixão, Sulfonated dendritic mesoporous silica nanospheres: a metal-free Lewis acid catalyst for the upgrading of carbohydrates, *Green Chem.*, 2020, **22**, 1754–1762.
49 C.-H. Kuo, A. S. Poyraz, L. Jin, Y. Meng, L. Pahalagedara, S.-Y. Chen, D. A. Kriz, C. Guild, A. Gudz and S. L. Suib, Heterogeneous acidic TiO_2 nanoparticles for efficient conversion of biomass derived carbohydrates, *Green Chem.*, 2014, **16**, 785–791.
50 G. Morales, A. Osatiashtiani, B. Hernández, J. Iglesias, J. A. Melero, M. Paniagua, D. Robert Brown, M. Granollers, A. F. Lee and K. Wilson, Conformal sulfated zirconia monolayer catalysts for the one-pot synthesis of ethyl levulinate from glucose, *Chem. Commun.*, 2014, **50**, 11742–11745.
51 L. Peng, L. Lin, J. Zhang, J. Shi and S. Liu, Solid acid catalyzed glucose conversion to ethyl levulinate, *Appl. Catal., A*, 2011, **397**, 259–265.
52 S. Quereshi, E. Ahmad, K. K. K. Pant and S. Dutta, Insights into Microwave-Assisted Synthesis of 5-Ethoxymethylfurfural and Ethyl Levulinate Using Tungsten Disulfide as a Catalyst, *ACS Sustainable Chem. Eng.*, 2020, **8**, 1721–1729.
53 Z. Zhang and H. Yuan, An alumina-coated UiO-66 nanocrystalline solid superacid with high acid density as a catalyst for ethyl levulinate synthesis, *J. Chem. Technol. Biotechnol.*, 2020, **95**, 2930–2942.
54 P. H. Pfromm, V. Amanor-Boadu, R. Nelson, P. Vadlani and R. Madl, Bio-butanol vs. bio-ethanol: A technical and economic assessment for corn and switchgrass fermented by

yeast or Clostridium acetobutylicum, *Biomass Bioenergy*, 2010, **34**, 515–524.

55 M. Mascal and E. B. Nikitin, Comment on Processes for the Direct Conversion of Cellulose or Cellulosic Biomass into Levulinate Esters, *ChemSusChem*, 2010, **3**, 1349–1351.

56 W. Zhu, C. Chang, C. Ma and F. Du, Kinetics of Glucose Ethanolysis Catalyzed by Extremely Low Sulfuric Acid in Ethanol Medium, *Chin. J. Chem. Eng.*, 2014, **22**, 238–242.

57 N. Shi, Q. Liu, H. Cen, R. Ju, X. He and L. Ma, Formation of humins during degradation of carbohydrates and furfural derivatives in various solvents, *Biomass Convers. Biorefin.*, 2020, **10**, 277–287.

58 X. Hu, C. Lievens, A. Larcher and C.-Z. Li, Reaction pathways of glucose during esterification: Effects of reaction parameters on the formation of humin type polymers, *Bioresour. Technol.*, 2011, **102**, 10104–10113.

59 T. Flannelly, S. Dooley and J. J. Leahy, Reaction Pathway Analysis of Ethyl Levulinate and 5-Ethoxymethylfurfural from D-Fructose Acid Hydrolysis in Ethanol, *Energy Fuels*, 2015, **29**, 7554–7565.

60 S. Wang, Y. Chen, Y. Jia, G. Xu, C. Chang, Q. Guo, H. Tao, C. Zou and K. Li, Experimental and theoretical studies on glucose conversion in ethanol solution to 5-ethoxymethylfurfural and ethyl levulinate catalyzed by a Brønsted acid, *Phys. Chem. Chem. Phys.*, 2021, **23**, 19729–19739.

61 M. Howard, *Real Reaction Kinetics for the Production and Utilisation of Advanced Biofuels*, Department of Chemical Sciences, University of Limerick, 2019.

62 M. Pointner, P. Kuttner, T. Obrlik, A. Jager and H. Kahr, Composition of corncobs as a substrate for fermentation of biofuels, *Agronomy Res.*, 2014, **12**, 391–396.

63 J. Zhang, T. Chen, J. Wu and J. Wu, A novel Gaussian-DAEM-reaction model for the pyrolysis of cellulose, hemicellulose and lignin, *RSC Adv.*, 2014, **4**, 17513.

64 E. Ranzi, A. Cuoci, T. Faravelli, A. Frassoldati, G. Migliavacca, S. Pierucci and S. Sommariva, Chemical Kinetics of Biomass Pyrolysis, *Energy Fuels*, 2008, **22**, 4292–4300.

65 M. Kelly, M. Fortune, G. Bourque and S. Dooley, Machine learned compact kinetic models for methane combustion, *Combust. Flame*, 2023, **253**, 112755.

66 M. K. Ghosh, M. S. Howard, K. Dussan and S. Dooley, Mechanism and theory of D-glucopyranose homogeneous acid catalysis in the aqueous solution phase, *Phys. Chem. Chem. Phys.*, 2019, **21**, 17993–18011.

67 K. Sun, L. Zhang, Y. Shao, Q. Li, H. Fan, G. Gao, S. Zhang, Q. Liu, Y. Wang and X. Hu, Conversion of monosaccharides into levulinic acid/esters: impacts of metal sulfate addition and the reaction medium, *J. Chem. Technol. Biotechnol.*, 2019, **94**, 3676–3686.

68 F. Lai, F. Yan, P. Wang, F. Qu, X. Shen and Z. Zhang, Efficient one-pot synthesis of ethyl levulinate from carbohydrates catalyzed by Wells-Dawson heteropolyacid supported on Ce–Si pillared montmorillonite, *J. Cleaner Prod.*, 2021, **324**, 129276.

69 S. Wang, Y. Chen, Y. Jia, C. Wang, G. Xu, Y. Jiao, C. He, C. Chang and Q. Guo, DFT and dynamic analysis of glucose alcoholysis conversion to 5-ethoxymethylfurfural and ethyl levulinate, *Fuel*, 2022, **326**, 125075.

70 S. Zhao, G. Xu, J. Chang, C. Chang, J. Bai, S. Fang and Z. Liu, Direct Production of Ethyl Levulinate from Carbohydrates Catalyzed by H-ZSM-5 Supported Phosphotungstic Acid, *BioResources*, 2015, **10**(2), 2223–2234.

71 L. Zhang, L. Tian, Z. Xu and L. Wang, Direct production of ethyl levulinate from carbohydrates and biomass waste catalyzed by modified porous silica with multiple acid sites, *Process Biochem.*, 2022, **121**, 152–162.

72 E. S. Olson, M. R. Kjelden, A. J. Schlag and R. K. Sharma, Levulinate Esters from Biomass Wastes, Chemicals and Materials from Renewable Resources, *J. Am. Chem. Soc.*, 2001, 51–63.

73 J. Tan, Q. Liu, L. Chen, T. Wang, L. Ma and G. Chen, Efficient production of ethyl levulinate from cassava over $Al_2(SO_4)_3$ catalyst in ethanol–water system, *J. Energy Chem.*, 2017, **26**, 115–120.

74 R. Le Van Mao, Q. Zhao, G. Dima and D. Petraccone, New Process for the Acid-Catalyzed Conversion of Cellulosic Biomass (AC3B) into Alkyl Levulinates and Other Esters Using a Unique One-Pot System of Reaction and Product Extraction, *Catal. Lett.*, 2011, **141**, 271–276.

75 Y. Zhang, X. Wang, T. Hou, H. Liu, L. Han and W. Xiao, Efficient microwave-assisted production of biofuel ethyl levulinate from corn stover in ethanol medium, *J. Energy Chem.*, 2018, **27**, 890–897.

76 C. Chang, G. Xu and X. Jiang, Production of ethyl levulinate by direct conversion of wheat straw in ethanol media, *Bioresour. Technol.*, 2012, **121**, 93–99.

77 T. Zhao, Y. Zhang, G. Zhao, X. Chen, L. Han and W. Xiao, Impact of biomass feedstock variability on acid-catalyzed alcoholysis performance, *Fuel Process. Technol.*, 2018, **180**, 14–22.

78 L. di Bitonto, G. Antonopoulou, C. Braguglia, C. Campanale, A. Gallipoli, G. Lyberatos, I. Ntaikou and C. Pastore, Lewis-Brønsted acid catalysed ethanolysis of the organic fraction of municipal solid waste for efficient production of biofuels, *Bioresour. Technol.*, 2018, **266**, 297–305.

79 H. Rizqullah, J. Yang and J. W. Lee, Temperature-swing transesterification for the coproduction of biodiesel and ethyl levulinate from spent coffee grounds, *Korean J. Chem. Eng.*, 2022, **39**, 2754–2763.

80 J. Yang, J. Park, J. Son, B. Kim and J. W. Lee, Enhanced ethyl levulinate production from citrus peels through an in-situ hydrothermal reaction, *Bioresour. Technol. Rep.*, 2018, **2**, 84–87.

81 C. Ming, K. Sun, Y. Shao, Z. Zhang, S. Zhang, Q. Liu, Y. Wang, S. Hu, J. Xiang and X. Hu, Conversion of Cellulose to Levulinic Acid/Ester over an Acid Catalyst: Impacts of Dispersion of Hydrogen Ions on Polymerization Reactions, *Energy Fuels*, 2019, **33**, 11187–11199.

82 C. Gong, J. Wei, X. Tang, X. Zeng, Y. Sun and L. Lin, Production of levulinic acid and ethyl levulinate from cellulosic pulp derived from the cooking of lignocellulosic biomass with active oxygen and solid alkali, *Korean J. Chem. Eng.*, 2019, **36**, 740–752.